

Bachelor Thesis

Optimal Mitigation under Carbon Cycle Feedbacks

**Department of Business Administration
(Quantitative Business Administration)
University of Zurich**

Anna-Mateja Delas

Contact Details:	anna-mateja@delas.ch Untere Bühlenstrasse 111 8708 Männedorf
Student ID:	07-740-764
Subject:	Economics
Supervisor:	Dr. Thomas S. Lontzek
Deadline:	August 26, 2011

Abstract

In most climate-economy models the atmospheric rate of decay is constant. However, because of climate change positive carbon cycle feedbacks dampen the natural absorption rate of the continental and marine ecosystems. As climate change affects the global economy (i.e., represented by GDP), developing an accurate model of the atmospheric rate of decay becomes increasingly important in optimizing the economic and social decisions concerning consumption, investment and mitigation. A Ramsey-like growth model assuming continuous time, with an infinite time horizon and a deterministic analysis is used to investigate and the current Hamiltonian approach of optimal control theory set up. The model endogenously incorporates the environmental externalities as linearly fitted relative decay rate functions with a negative slope, and accordingly concave absolute decay change rates which suggest an inverted U-shape. Because of the model's multidimensional character, a numerical procedure is inevitable. What follows, inter alia, are the steady states and the simulation of optimal time paths for the control variables consumption and mitigation, and the state variables atmospheric stock of carbon and capital stock. Those are evaluated for three major SRES projections published by the IPCC, as well as for the CJK carbon projection, which is another relevant integrated assessment model. A deeper focus is set on the variable mitigation.

Contents

List of Figures	III
1 Introduction	1
2 Climate change	3
3 Atmospheric decay of CO₂	6
3.1 Historic data of atmospheric carbon growth and decay	6
3.2 Future carbon projections of decay functions	11
3.3 Functional decay forms	17
4 The model	19
5 Results	25
5.1 SRES projections	26
5.2 CJL projection	30
6 Conclusion	32
References	33

List of Figures

1	Atmospheric stock of carbon (S_t) in ppm over time t (1959 - 2008)	6
2	Atmospheric absolute decay rate $B(S_t)^{1959-2008}$ in GtC for any given atmospheric stock change level ($S_t - S_{pi}$)	8
3	Atmospheric relative decay rate $\beta(S_t - S_{pi})^{1959-2008}$ as a decimal number (ratio) for any given atmospheric stock change level ($S_t - S_{pi}$)	9
4	Relative decay rates $\beta(S_t - S_{pi})$ as a decimal number (ratio) for any given atmospheric stock change level ($S_t - S_{pi}$) for SRES . . .	12
5	Fitted relative decay rates $\beta(S_t - S_{pi})$ as a decimal number (ratio) for any given atmospheric stock change level ($S_t - S_{pi}$) for SRES .	13
6	Fitted relative decay rates $\beta(S_t - S_{pi})$ as a decimal number (ratio) for any given atmospheric stock change level ($S_t - S_{pi}$) for CJL, DICE and the historic data	16
7	Fitted absolute decay rate $B(S_t - S_{pi})$ in GtC for any given atmospheric stock change level ($S_t - S_{pi}$) for CJL	16
8	Optimal time paths $A_t^* \forall A \in S, K, \lambda_S, \lambda_K, C, I$ for any given time t for SRES. S is given in GtC; K, C, I are given in units of output; λ_S, λ_K are dimensionless. The coloured curves help to distinguish between B1, A1B and A1FI.	28
9	Optimal mitigation m_t^* as a decimal number (ratio) for any given time t for SRES	29
10	Optimal allocation $\xi_{M(m)}(t)^*$ as a decimal number (ratio) for any given time t for SRES	29
11	Optimal allocations $\xi_C(t)^*$ and $\xi_I(t)^*$ as a decimal number (ratio) for any given time t for SRES	29
12	Optimal time paths $A_t^* \forall A \in S, K, \lambda_S, \lambda_K, C, I$ for any given time t for CJL. S is given in GtC; K, C, I are given in units of output; λ_S, λ_K are dimensionless.	30
13	Optimal mitigation m_t^* as a decimal number (ratio) for any given time t for CJL	31

14	Optimal allocation $\xi_{M(m)}(t)^*$ as a decimal number (ratio) for any given time t for CJL	31
15	Optimal allocations $\xi_C(t)^*$ and $\xi_I(t)^*$ as a decimal number (ratio) for any given time t for CJL	31

1 Introduction

In a world where “sustainability” is becoming more and more important, the need to control the levels of pollution is crucial, or in mathematical terms, to apply optimal control theory and sustainable development to the net emissions less the decay of the pollution level [e.g., Hediger, 2009; Tahvonen and Salo, 1996].

Historically, we see that concerns of sustainability have already been a matter of grave importance in the Brundtland report of 1986, which formed the fundamental concept of sustainable development. This report basically says that the needs of the current generation have to be satisfied in a way where the needs of the next generation are not compromised. Economic approaches to sustainability are founded on the main contributions from the early 1970’s [e.g., Daly, 1974; Hartwick, 1977; Solow, 1974] and the focus has been on the meaning of sustainability ever since. If we consider the current carbon dioxide emissions, we notice a heavy external factor on the future emissions’ social costs. However, letting a constancy-like-property be implemented, would result in constancy between periods. This would not be applicable to reality, as there would always be at least some damage caused by economic growth. Substitution between present and future utility has to be allowed, therefore a sustainability-like-property should be introduced instead. As Weitzman [2003, p. 246] formulates, discounted utilitarianism represents the most suitable form and can be characterized by: “The maximum amount that can presently be consumed without compromising future ability to consume at the same level.”

Nowadays, comprehensive calculations can be explored with the tools of dynamic optimization theory, in particular, with the current-value Hamiltonian function. As a long-run system, consisting of multiple periods of net investment and consumption, is considered, the comprehensive calculations combine the present with the future, which incorporates the sustainable character (i.e., future consumption). The relevant classical topics such as cost-benefit-analysis, consumer surplus and also the insights from price deflation can be put into more sustainable light by integrating the comprehensive analysis. Now, if every single

source of economic growth (i.e., natural resources, human capital) is captured by a certain form of capital, then everything affecting utility and therefore affecting social welfare, could be quantified as a vector of consumption, investment and mitigation. Therefore, a principle of sustainability could be stated as the sum of all constantly discounted utilities, which would equal dynamic welfare, together with the monetary value of consumption, which would equal discounted current, stationary-equivalent sustainable utility in order to increase utility or social welfare [Weitzman, 2003]. This principle proposes the maximization of the integral of discounted social utility, where a reflection on intertemporal welfare can be executed. Consumption would reflect the instantaneous utility; whereas, investment would reflect how current activities of the economy affect future utility. Similarly, Hartwick [1977] concludes that net investments would equal zero, if society invested all gains from an exhaustible resource pool back into a reusable capital pool, then, the maintenance of the sustainable-equivalent utility would be achieved. Thus, a net-zero investment rule sheds light on an intertemporal path of optimal pollution accumulation; however, such a “compensating” investment is not fulfilled in reality. There is a great overexploitation of fossil fuels worldwide, which has lead to extremely high carbon dioxide emission levels today compared to the pre-industrial ones. Besides the burning of fossil fuels¹, negative impacts on the global carbon cycle are also caused by deforestation (i.e., changes in land use), cement manufacturing as well as gas flaring. The carbon cycle is put out of balance² in such a way that causes severe consequences like climate change and irreversible environmental damage.

The aim of the following thesis is to examine the atmospheric decay rate in greater detail. A function, which implies the negative effect of rising atmospheric stock levels is investigated. This type of modelling of the natural absorption rate allows one to set up a model, which is more realistic, and allows one to explore

¹When burnt, 1 kg Carbon (C) will release 3.67 kg of CO₂.

²Note, not only CO₂ is a powerful greenhouse gas which puts the carbon cycle out of balance, but also water vapor, methane, laughing gas (nitrous oxide), ozone and human-caused non-CO₂-gases like per- and hydrofluorocarbons or sulphur hexafluoride.

the results more carefully.

We proceed as follows: In the next section an overview of the climate change problem is presented. Section 3 approximates reasonable fits for specific types of carbon projections. Section 4 introduces the model, and section 5 presents the results. Subsequently, section 6 concludes by discussing the results and their global implications.

2 Climate change

If, since the industrial revolution, all anthropogenic CO₂ emissions had stayed in the atmosphere, the global warming would have already had an enormous impact on our planet. However, such a scenario has not yet occurred, as there exist fluxes between the atmosphere and the natural reservoirs (i.e., carbon sinks) which remove the carbon from the atmosphere such as the ocean, and land or undisturbed tropical forests [IPCC, 2007]. These dynamic fluctuations are referred to the global carbon cycle and research has tried to capture this in coupled climate models. The flow of the ocean sinks is around 25% of the human-caused CO₂ per year [Canadell et al., 2007]. In recent time, the dissolution of carbon dioxide has impaired water chemistry of the ocean. This leads to a decomposition of carbonate ions and has caused many important marine organisms to die such as corals and sea shells, which bind CO₂ through sedimentation. As a result, the buffer capacity of the ocean declines and weakens the transformation of carbon dioxide into nongaseous compounds like carbonate ions, carbonic acid and bicarbonate. Furthermore, the thermal expansion of the deep sea entails the evaporation of the frozen methane-hydrate, which in turn releases another greenhouse gas (i.e., methane, which is even more destructive than carbon dioxide) [IPCC, 2007]. The land has taken up approximately 30% of the annual anthropogenic emissions³ [Canadell et al., 2007] and the terrestrial mechanisms suggest

³However, if we look at the atmospheric stock accumulated rather than the flow rate, the marine ecosystem is attributed to be the the largest non-atmospheric carbon sink. On the contrary, if we look at the atmospheric flow rate, the terrestrial biota shows a larger one.

that the higher CO₂ concentration improves the photosynthesis (i.e., fertilization effect) of plants and trees. This is actually the only negative feedback loop, and counteracts the multiplicity of positive feedback effects; however, this effect only lasts as long as the terrestrial biota lives. As soon as the plants decompose, they release the absorbed carbon dioxide and making forests temporary carbon sinks. The increasing deforestation, on the other hand, worsens the photosynthesis. Examples of positive (reinforcing) carbon-cycle feedbacks are the melting of the permafrost soils, the albedo decreases, as well as the higher water vapor concentrations in the atmosphere. History suggests that these feedback loops have been the most probable reason for major shifts in the climates (e.g., the great ice age). Last, but not least, the change in the observed average global surface temperature between the warm age and the ice age is around 5° Celsius only [Holdren, 2008]. Such a margin seems small to alter an entire climate system, especially, if the consensus target implies a temperature increase of 2° Celsius.

Empirical research proves that positive carbon-cycle feedbacks lessen the potential of CO₂ absorption of natural carbon sinks⁴ [e.g., Cox et al., 2000; Friedlingstein et al., 2006; Fung et al., 2005; Knutti et al., 2006; 2005; Raupach et al., 2008; Sarmiento et al., 1998]. If more CO₂ is emitted, a rise in temperature (i.e., climate change) will go along with it. This results in a weaker natural uptake of the greenhouse gas. If we look at the ocean, we see that with higher temperatures, the carbon uptake capacity declines [IPCC, 2007]. The carbon sink is not able to absorb in unconstrained amounts and therefore “the greater the level of pollution, the greater is nature’s capacity of assimilation” [Comolli, 1977, p. 291] does not work [e.g., Comolli, 1977; Dasgupta, 1982; Forster, 1975; Tahvonen and Salo, 1996]. There are highly nonlinear interactions happening in the climate system [Sokolov et al., 1998]. The natural sinks, which absorb the “missing

⁴The land sinks have not changed much since 1958/59. Remember that they feature an annual absorption of $\approx 30\%$. They will hopefully not change in the future. The great damage is seen in the ocean sinks, where the oceanic absorption has shown a drastic decline since 1958/59. Whereas the removal flow was $>30\%$ fifty years ago, it now ranges between $20 - 25\%$, suggesting a saturation ceiling on the upper front. Similarly to the results of Canadell et al. [2007], Solomon et al. [2007] predict a further 30%-removal of the atmospheric stock within the next few centuries and only 20% are suggested to accumulate eventually in the atmosphere.

carbon”, as the decay of carbon dioxide is often referred to, change over time as a reply to climate change. An increase in the long-term (50-year) airborne fraction⁵, which essentially describes the ratio between the annual expansion in atmospheric carbon dioxide and the annual anthropogenic emissions owing to physical and biological processes, leads to a decreased efficiency of the sinks and therefore lessens their ability to absorb the human-induced emissions [Canadell et al., 2007].

The climate change debate has often been formulated as a problem of how to make the concentration of atmospheric carbon stable at a reasonable rate; say, to allow a temperature increase of 2° Celsius compared to the preindustrial level. The question concerns the emitted amount of CO₂, which maximally enables nature to stay below such a temperature ceiling. Technically, the stabilization at an atmospheric level of 550 parts per million would be feasible. Better technology options are possibilities to handle the climate change problem. Those consist of the improvement of energy efficiency, renewable energy, the reduction of non-CO₂ green house gases, the stop of the deforestation, etc. [Moomaw et al., 2001; Metz and van Vuuren, 2006]. Decarbonization in the energy-supply also states an option (e.g., the use of wind, solar, gas technologies), and specifically includes the CCS (carbon capture and storage), or the storage in the deep ocean. In general, carbon sequestration can be viewed as the process of cutting back carbon from the atmosphere and placing it in a reservoir [e.g., Lackner, 2003].⁶ Such a term is often referred to the idea of mitigating CO₂ and shows how human kind could intervene in the carbon cycle process.⁷

⁵I.e., airborne fraction equals the quotient of annual total emissions less the (annual) natural uptake relative to the annual total emissions, or the atmospheric CO₂ level in the current year less the atmospheric CO₂ level in the previous year relative to the total annual emissions (that is how much of the annual total emissions relatively accumulate in the atmosphere per year).

⁶However, “artificial” sinks such as landfills and geological storage sites are usually much smaller than the natural carbon sinks (i.e., ocean and terrestrial biota).

⁷At this point it is worth mentioning that mitigating CO₂ and capturing CO₂ is not the same. The mitigation cost is not the mere sum of its elements such as capture, transport or storage, as IPCC [2007] specifies. The reason lies in the difference of the captured CO₂ level and the avoidance of an increase in the atmospheric CO₂ level. The distinction between the terms of the CO₂ level’s basis should be made (i.e., whether it is an avoided or a captured basis) and thus mitigation costs are best characterized by avoided costs.

3 Atmospheric decay of CO₂

3.1 Historic data of atmospheric carbon growth and decay

In the last 250 years, since the beginning of the industrial revolution, the atmospheric CO₂ level has risen from ~ 285 (measured by air bubbles) to 394 parts per million⁸ (status: June, 2011). Since 1958/59, the Mauna Loa observatory in Hawaii measures the atmospheric CO₂ concentration on a daily basis. It is the longest record of continuous monitoring which exists [NOAA1, NOAA2].

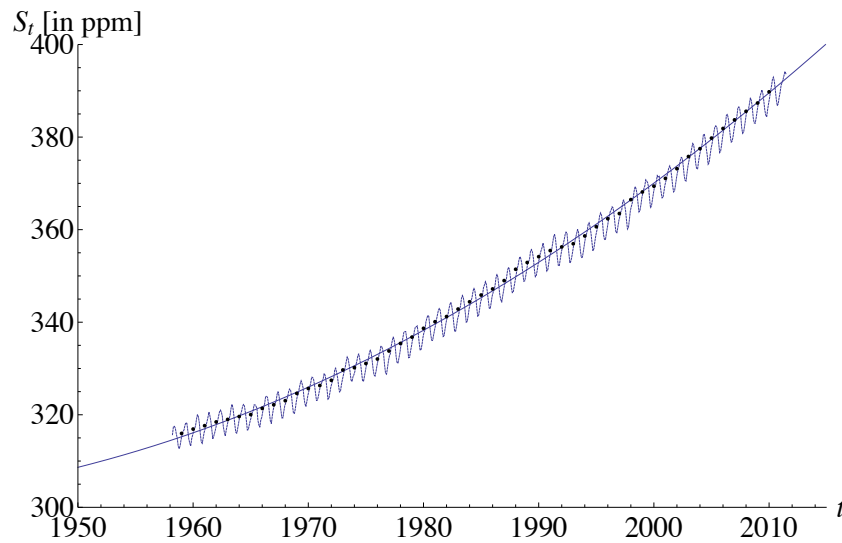


Figure 1: Atmospheric stock of carbon (S_t) in ppm over time t (1959 - 2008)

Figure 1 illustrates the atmospheric carbon stock and its development through time. The dots indicate the annually measured stocks, whereas the dashed curve refers to the seasonal winter and summer variability. There is an exponential trend estimated, if emissions continue to grow in the future.⁹

Parallel to atmospheric observations, data is available on the annual emissions from fossil fuel combustion and deforestation. From 1958 up to 2008 total emissions have been around 5.4 PgC (GtC) on average [CDIAC]. At the moment,

⁸2.124 PgC (petagrams of carbon, where 1 Pg = 1 Gigaton (Gt) = 10^{15} g) equal 1 ppm (part/s per million) of CO₂. Note from earlier, 1 kg C \sim 3.67 kg CO₂. Therefore, it holds that 1 PgC \sim 3.67 Gt CO₂.

⁹The non-linear trend $44948.4 - 46.41t + 0.012t^2$ is significant and contains a p-value $< 6.810 \cdot 10^{-29}$ for every fitted estimate and a sum of squares for error (SSE) equal to 21.7.

the annual total CO₂ emissions amount to 9 - 10 PgC. Almost one half of the annual emissions accumulate in the atmosphere, suggesting the present airborne fraction (a) to be $\sim 50\%$.¹⁰ In correspondence, the natural sinks have absorbed $(1 - a)\%$ of the human-induced emissions. Though, only measurements over the atmospheric CO₂ levels can be made. The scientific lack in knowledge in measuring the annual CO₂ budget of the carbon sinks can presently not be overcome, and the quantification about land and ocean sinks are not sufficiently accurate [Le Quéré et al., 2009]. The trajectory of the atmospheric CO₂ concentrations over time represents the impact of the sinks and therefore their removal speed (i.e., transfer velocity) [Battle et al., 2000; Francey et al., 1995; Rayner et al., 1999].

However, the atmospheric absorption, has varied substantially, whilst the total emissions have not. The latter shows a rise over the long term but does not necessarily entail any large year-to-year variation like the carbon uptake from the oceanic and terrestrial biota. There is an atmospheric uptake variation of approximately ± 2 PgC per year [Quay, 2002]. Similarly, Canadell et al. [2007] compile an uncertainty of ± 0.4 PgC per year for the ocean sink, and an uncertainty of ± 0.7 PgC per year for the land sink, suggesting an uncertainty of ~ 0.6 PgC for both sinks (because of dependent probabilities). Since 1958/59, the airborne fraction has ranged from 0 - 0.8 [Canadell et al., 2007]. This indicates uncertainty and thus a stochastic process in the ecosystem [Le Quéré et al., 2009]. The year-to-year variability suggests being due to terrestrial uptake rather than oceanic uptake [Quay, 2002]. The large interannual variability in land sinks is driven by changes in precipitation, temperature of the land surface, as well as radiation [Mercado et al., 2009; Peylin et al., 2005; Sitch et al., 2008], whilst the small interannual variability in ocean sinks is driven by El Niño and La Niña

¹⁰Le Quéré et al. [2009] report an airborne fraction (a) of 43% on average over the years 1959 - 2008 (with an increase rate of $0.3 \pm 0.2\%$). Moreover, the airborne fraction has changed from 40% to 45% for the last 50 years. Thus, the natural sink's uptake efficiency has declined by 5% due to climate change and variation. Canadell et al. [2007] report a proportional trend in the airborne fraction $[(a^{-1})da/dt]$ over the period 1959 - 2006 as an estimate of $+0.25 \pm 0.0021$ per year.

states.¹¹ Furthermore, by each unit of carbon dioxide emitted, the ability to take up the green house gas declines as the sinks possibly contain a saturation ceiling.¹² Such a ceiling induces a concave function of the atmospheric absolute decay rate, which is indicated by $B(S_t)^{1959-2008}$ in Figure 2.¹³

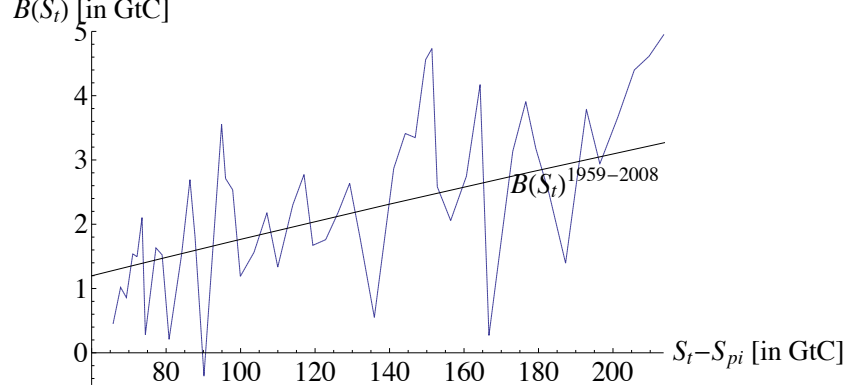


Figure 2: Atmospheric absolute decay rate $B(S_t)^{1959-2008}$ in GtC for any given atmospheric stock change level $(S_t - S_{pi})$

The x-axis represents the change in atmospheric carbon stock compared to the preindustrial level of 605.34 GtC (~ 285 ppm) $(S_t - S_{pi})$ at a given time, whilst the y-axis shows the absolute atmospheric decay rate $B(S_t)$. From now on, units are always given in gigatons of carbon rather than parts per million. An implied absolute decay rate $B(S_t)$ (or similarly $B(S_t - S_{pi})$)¹⁴ comes from the following equation

$$S_{t+1} = S_t + E_t - B(S_t) \quad (1)$$

where E_t entail the emissions at a given time.

¹¹Results from 2008 (i.e., then-prevalent El Niño/Southern Oscillation was positive, hence in a La Niña condition) point out the change in the absorption rate to be larger for the forests than for the oceans, where the La Niña circumstance improved the efficiency of the terrestrial sinks more than it impaired the efficiency of the ocean sinks [Le Quéré et al., 2009].

¹²E.g., the capacity of the ocean sink is restricted compared to fossil fuels [Lackner, 2002].

¹³ $B(S_t)^{1959-2008}$ equals to $0.3074 + 0.0152(S_t - S_{pi}) - 6.3913 \cdot 10^{-6}(S_t - S_{pi})^2$ and holds a p-value $< 2.6 \cdot 10^{-94}$ for every fitted estimate with a SSE ~ 0.011 .

¹⁴There is a difference between the both as $B(S_t)$ entails the measured absolute decay, whereas $B(S_t - S_{pi})$ refers to the function of a fitted *beta* (i.e., relative decay rate $\beta(S_t - S_{pi})$), which will be introduced together with the CJL scenario later) multiplied by $(S_t - S_{pi})$. In the modelling part of section 4 $B(S_t - S_{pi})$ will be used.

One should be aware that the fitted $B(S_t)^{1959-2008}$ function refers from highly variable data (i.e., CO₂ uncertainty). It would also be possible to fit any function across the historic data; either a linear or even an exponentially rising one. The advantage of the concave function allows one to use a pessimistic and thus a more risk averse perspective over the sinks' capacity to absorb CO₂. Moreover, it goes hand in hand with the various *beta*-projections for the future, and represents the functional forms suggested by literature.¹⁵ Notice in Figure 2 the negative value -0.36 [GtC] for $B(S_t)^{1959-2008}$ at $(S_t - S_{pi}) = 90.16$ [GtC]. This proposes that the oceans and terrestrial biota could have behaved as a net source of carbon¹⁶ rather than a net sink in this specific year (i.e., 1972 in line with the oil crisis), and elucidates that the sum of S_t (i.e., S_{1972}) and E_t (i.e., E_{1972}) is smaller than S_{t+1} (i.e., S_{1973}).¹⁷

Figure 3 gives the corresponding relative decay rate (i.e., $\beta(S_t - S_{pi})$)¹⁸ in the y-axis.

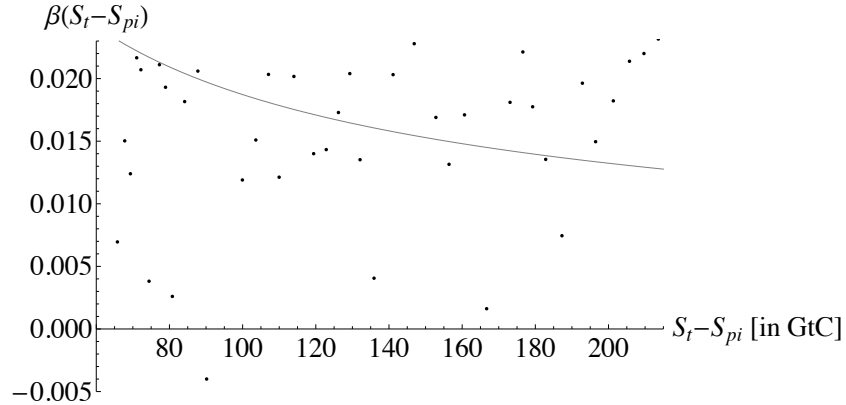


Figure 3: Atmospheric relative decay rate $\beta(S_t - S_{pi})^{1959-2008}$ as a decimal number (ratio) for any given atmospheric stock change level $(S_t - S_{pi})$

¹⁵E.g., see section 3.2 and 3.3 respectively.

¹⁶I.e., consult Heimann and Reichstein [2008] for a detailed discussion of the terrestrial biosphere under the impact of climate change.

¹⁷Note here that if we decrease or stop emissions E_t in the future in order to prevent a severe climate change, we should be conscious that the terrestrial and marine ecosystems themselves may eventually start emitting CO₂ and become substantial sources of carbon.

¹⁸ $\beta(S_t - S_{pi})^{1959-2008}$ equals to $0.187226 / (S_t - S_{pi})^{0.5}$ and holds a p-value of $1.826 \cdot 10^{-18}$ for the fitted estimate with a SSE ~ 0.004 . The estimated variance is 0.000081 and thus suggests a standard deviation of 0.00902.

It comes from

$$\beta(S_t - S_{pi}) = \frac{B(S_t)}{(S_t - S_{pi})} \quad (2)$$

Again, the dots denote the measured data from history. A magnifying airborne fraction goes along with the climate models, but the dimensions appear to be more significant and suggest a stronger-than-expected, and, furthermore, a sooner-than expected feedback loop (i.e., climate forcing), and accordingly an acceleration process in atmospheric CO₂ levels [Canadell et al., 2007]. This implies that human-caused emissions have grown faster than the ability of the sinks to store those. This results in an absorption rate, which is essentially slower than the rate at which emissions are pacing [Canadell et al., 2007]. Inferring a decay function of the carbon absorption, we conclude a non-constant, absolute decay (rate), with a non-linear relative decay rate.¹⁹ Note again: the higher the level of pollution, the lower nature’s ability to absorb the emitted CO₂, incorporating a decay rate at a slower pace.²⁰ If the atmospheric CO₂ growth (i.e., airborne fraction) is exponentially (i.e., convexly) increasing because of anthropogenic emissions, which are still rising rapidly owing to emerging economies such as China, and therefore the absolute decay rate concavely rising, then the relative decay rate is convexly falling towards a rate of zero uptake with a higher pollution level²¹ (i.e., decrease of the net carbon uptake and in the extreme case the reversal to a net carbon source). This suggests an acceleration in the atmospheric growth and a stronger convexity in Figure 1. A function of rapidly increasing emissions, and thus a rapidly increasing atmospheric CO₂ growth, is closest to the current trend, which complicates the challenge to stabilize the atmospheric CO₂ concentration [Nakicenović and Swart, 2000].

¹⁹However, the relative rate of decay we conduct is linearly fitted.

²⁰I.e., due to an ever-increasing rate of anthropogenic emissions, the “average” natural removal “rate” increases as well, but at a slower pace.

²¹Imagine the relative decay rate to be all the secants, which go through the origin. Thus the slopes of the secants are falling with higher $(S_t - S_{pi})$. Similarly, the marginal decay rate refers to all the tangents. Their slopes are falling, as well. Note also, that it is important to use the atmospheric stock change compared to the preindustrial stock level in order to avoid relative rates to show a strange behaviour because of a negative axis intercept.

3.2 Future carbon projections of decay functions

The non-linear rate of decay incorporates an airborne fraction projecting a positive trend. Le Quéré et al. [2009] provide four possible reasons (i) - (iv) for a positive progression. Regulating the absorption rate of the natural sinks takes longer than the fast increases in atmospheric CO₂ levels (i). Also, the natural sinks respond to climate changes and thus to positive climate cycle feedback loops (ii) (e.g., less carbonate ions in the ocean sink, deforestation leading to a smaller terrestrial sink with less plants and trees). Furthermore, the efficiency of the natural sinks is likely to deteriorate because of boundaries in land or ocean fertilization (iii). Even if society tries to offset the rising effect with ocean fertilization (eutrophication), the carbon cycle effects as amplifiers of future warming still operate in a strong way [Matthews and Keith, 2007]. Last, but not least, processes of still “unknown” sinks having the character of a residual, which are not included in current modeling, could lead to an increasing airborne fraction (iv) [Denman et al., 2007].

Estimating the carbon trajectory for the future is essential as it tries to evaluate all possible scenarios given specified circumstances. The IPCC came up with a detailed set of scenarios called “Special Report on Emissions Scenarios” (SRES). Those were built to examine the impacts of different emission outputs and to assess the future environmental development. They are divided by three components: the storyline, scenario and scenario family. There consist four storylines (i.e., A1, A2, B1, B2) and each set, either A or B, is weighed against contrasting trends [Nakicenović and Swart, 2000]. In the following, three scenarios from SRES were chosen to be presented:²² the fossil fuel intensive A1FI (worst case), the across energy sources balanced A1B (middle case) and the environmentally clean B1 (best case).

The IPCC [*SRES*] defines the A1FI & A1B scenario as follows: “A future world of very rapid economic growth, low population growth and rapid introduction of new and more efficient technology. Major underlying themes are economic

²²To date, around 40 scenarios have been assessed. All scenarios are equally likely to happen.

and cultural convergence and capacity building, with a substantial reduction in regional differences in per capita income. In this world, people pursue personal wealth rather than environmental quality.”²³

The B1, on the contrary, is defined as: “A convergent world with the same global population as in the A1²⁴ storyline but with rapid changes in economic structures toward a service and information economy, with reductions in materials intensity, and the introduction of clean and resource-efficient technologies.”

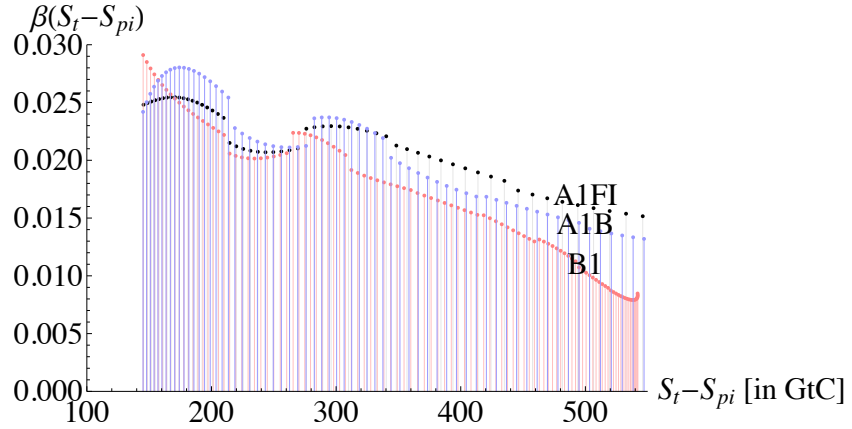


Figure 4: Relative decay rates $\beta(S_t - S_{pi})$ as a decimal number (ratio) for any given atmospheric stock change level ($S_t - S_{pi}$) for SRES

Figure 4 represents the three IPCC *beta*-projections. Data was provided by the Data Distribution centre of the IPCC [BERN].²⁵ B1 indicates the best relative rate of decay for lower stock levels, but highlights the worst one for higher stock levels. The exact vice-versa trend applies for A1FI. This is due to A1FI’s fossil fuel intensitivity. As the carbon emissions decline in B1, the relative rate of decay slows down and even suggests a tranformation from carbon sinks into carbon sources, whereas the latter is still forced to be at a higher value if the economy projects much carbon release as in A1FI. The A1B stands approximately between both extreme cases.

²³The A1FI and A1B are characterized by the same key assumptions. However, the difference lies in the energy sources (“fossil fuel intensive” versus “balanced”).

²⁴I.e., A1FI and A1B.

²⁵The projecting data was given in interannual intervalls of 10 years. Whilst the annual atmospheric stock data was adjusted through interpolation, the projecting data of the emissions was annually fitted with a function.

Figure 5 shows the same data as in figure 4; but now the projections are linearly fitted as functions.²⁶

To emphasize at which values the different SRES lines cross, A is given by $(186.7, 0.0248)$, B by $(245.1, 0.0221)$ and C by $(345.2, 0.0206)$.

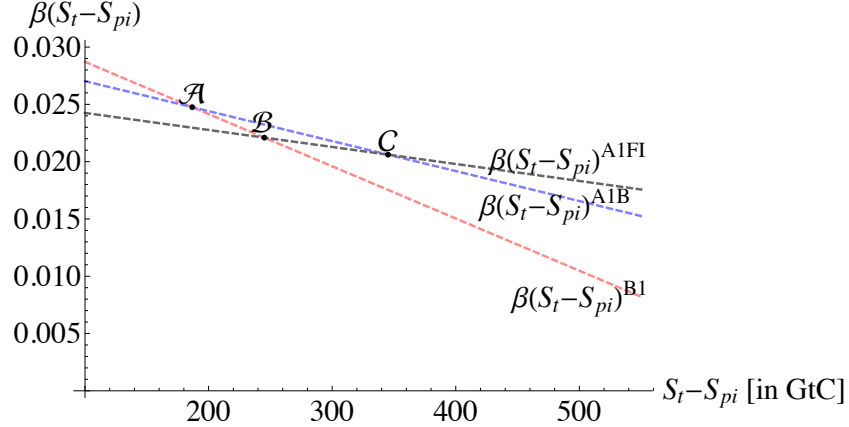


Figure 5: Fitted relative decay rates $\beta(S_t - S_{pi})$ as a decimal number (ratio) for any given atmospheric stock change level $(S_t - S_{pi})$ for SRES

The reason why SRES, and similarly other projecting models like DICE or the CJL model presented afterwards, shows a large difference (i.e., variance) between each other is very much due to the uncertainty involved in the climate system.²⁷ The effects of carbon-cycle feedbacks under uncertainty, in general, are an interesting part of prediction theory. The relationships between temperature, climate patterns and carbon emission concentrations are unsure and thus inherently stochastic [Pindyck, 2007; Sokolov et al., 1998]. The contingent decay of CO_2 leads to contingent atmospheric accumulation of the green house gas

²⁶ $\beta(S_t - S_{pi})^{B1}$ equals to $0.0333 - 0.000046(S_t - S_{pi})$ and holds a p-value $< 1.21 \cdot 10^{-81}$ for every fitted estimate with a SSE ~ 0.00013 . The estimated variance is $1.22 \cdot 10^{-6}$ and thus suggests a standard deviation of 0.0011. $\beta(S_t - S_{pi})^{A1B}$ equals to $0.0296 - 0.000026(S_t - S_{pi})$ and holds a p-value $< 2.15 \cdot 10^{-63}$ for every fitted estimate with a SSE ~ 0.00031 . The estimated variance is $2.85 \cdot 10^{-6}$ and thus suggests a standard deviation of 0.0017. $\beta(S_t - S_{pi})^{A1FI}$ equals to $0.0257 - 0.000015(S_t - S_{pi})$ and holds a p-value $< 1.25 \cdot 10^{-63}$ for every fitted estimate with a SSE ~ 0.00027 . The estimated variance is $2.5 \cdot 10^{-6}$ and thus suggests a standard deviation of 0.0016.

²⁷According to Golub et al. [2011] there exist two types of uncertainties: parametric uncertainty and stochasticity. The former emphasizes the insufficiencies related to specific parameters (e.g., how an increasing airborne fraction affects climate carbon cycle feedbacks). The latter emphasizes persistent climate randomness.

[Prentice et al., 2001]. Holding the carbon increase rate in the atmosphere fixed (i.e., the airborne fraction is not subject to uncertainty), the increase in climate temperature is highly ambiguous [e.g., Forest et al., 2006; Hegerl et al., 2006]. Especially, if there is used a coupled climate carbon model, which describes the interaction between the atmosphere and the ocean, a rise in extreme warming probabilities can be observed [Matthews and Keith, 2007]. In any event, uncertainty remains a main concern in climate change science. It alters the function of carbon decay. As warming probabilities vary, it is unsurprising for the annual airborne fraction to incorporate variability towards the upper front, as well. Reasons for the given uncertainty regard the behavior of the natural sinks, seismic instability and other variability (i.e., El Niño/La Niña for ocean sinks or precipitation for terrestrial sinks) [Jones and Cox, 2005]. Pyndick [2007] highlights three main uncertainty compounds; besides the ecological uncertainty, there also exist uncertainties over economic and technical changes. Economic uncertainty accounts for the uncertain economic directions of the future [Nakicenović and Swart, 2000]. Technical uncertainty includes the uncertain timing of the switch to renewable resources [e.g., Pommeret and Schubert, 2006; Schumacher, 2010]. In addition, mitigation policies with respect to their quantification remain uncertain as the linkage of human-induced emissions to atmospheric green house gas concentration on an interannual basis can be delayed by multiple years [Le Quéré et al., 2009].

Uncertainty is given in damage functions, consisting of environmental costs and benefits. Those are highly non-linear and a mere expected value analysis is not sufficient. Such functions incorporate irreversibilities and long-time horizons [Pindyck, 2007]. The first illuminates the fact that green house gas concentrations remain for many years in the atmosphere, and even if society radically decreased its emission levels, the atmospheric decay would still be slow-going.²⁸ The latter elucidates the case that uncertainty increases over longer periods of time (e.g.,

²⁸Only with sequestration, the rate of decay could be accelerated provided that emission levels stay low.

unclear discount rates).

Like SRES, *DICE* [developped by William D. Nordhaus, 2007] and *CJL* [i.e., Dynamic Stochastic General Equilibrium Analysis of Climate Change Policies and Discounting by Cai, Y., Judd, K. L. and Lontzek, T. S.] state another sort of integrated assesment models. These models have been put through by economists rather than climate change scientists. As DICE is only given in 10-year intervals and calculated with average values, the CJL model, which is basically the non-average extension of DICE, seems to be more accurate. Figure 6 depicts the relative decay rates for CJL, DICE, and the historic data. Note that the *beta*-function for the historic data set is only given in the corresponding time interval, whereas DICE and CJL are shown for a wider range of $(S_t - S_{pi})$ values.²⁹ The transition from the historic data to the CJL projection is very small and thus speaks for CJL's accuracy.³⁰ Inter alia, this is why the numerical analysis will be done for the CJL projecting model.³¹ Referring from $\beta(S_t - S_{pi})^{CJL}$, the relative projecting decay rate ranges from 1 - 2%.³²

What can be derived from the relative rate is the absolute change rate (e.g., for CJL as in figure 7).³³ The following equation illuminates this circumstance:

$$B(S_t - S_{pi}) = \beta(S_t - S_{pi}) \cdot (S_t - S_{pi}) \quad (3)$$

²⁹Compared to the IPCC projecting scenarios, DICE and CJL also show a wider range of $(S_t - S_{pi})$. This is due to their respective time projection horizon. A1FI, A1B and B1 are given for the years 1990 - 2090, whereas CJL and DICE are given for the years \sim 2007 - 2150.

³⁰However, keep in mind that we could have plotted any *beta*-function across the historic data. Maybe, we have just been lucky to obtain such a precision. In addition, $\beta(S_t - S_{pi})^{CJL}$ equals to $0.01668 - 7.88515 \cdot 10^{-6}(S_t - S_{pi})$ and holds a p-value $< 1.02154 \cdot 10^{-175}$ for every fitted estimate with a SSE $\sim 1.31 \cdot 10^{-6}$. The estimated variance is $8.896 \cdot 10^{-9}$ and thus suggests a standard deviation of 0.0000943. Furthermore, we do not want to fit one convex *beta*-function for CJL and the historic data together because the latter implies very large variance.

³¹Needlessly to say, the numerical analysis will also be done for the three IPCC scenarios as those present globally recognized integrated assessment models.

³²The relative decay rate is very small. This is due to the *x*-variable which defines the absolute change since the preindustrial stock concentration.

³³I.e., this shows $B(S_t - S_{pi})$ rather than $B(S_t)$.

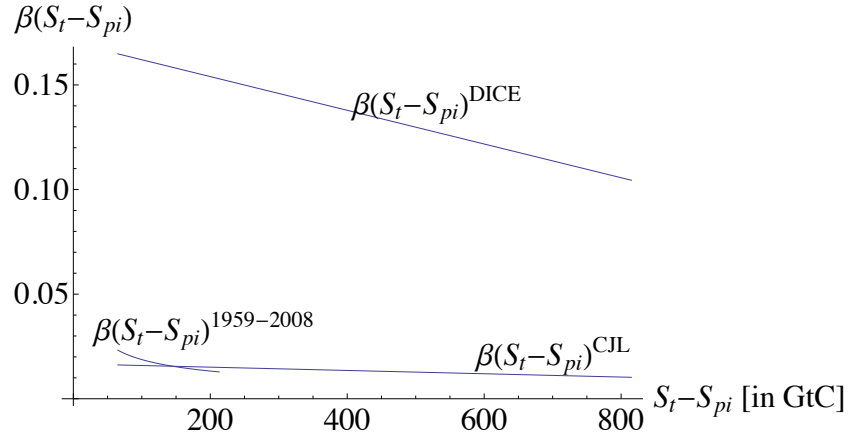


Figure 6: Fitted relative decay rates $\beta(S_t - S_{pi})$ as a decimal number (ratio) for any given atmospheric stock change level ($S_t - S_{pi}$) for CJL, DICE and the historic data

Such a B -function is presented in figure 7.³⁴

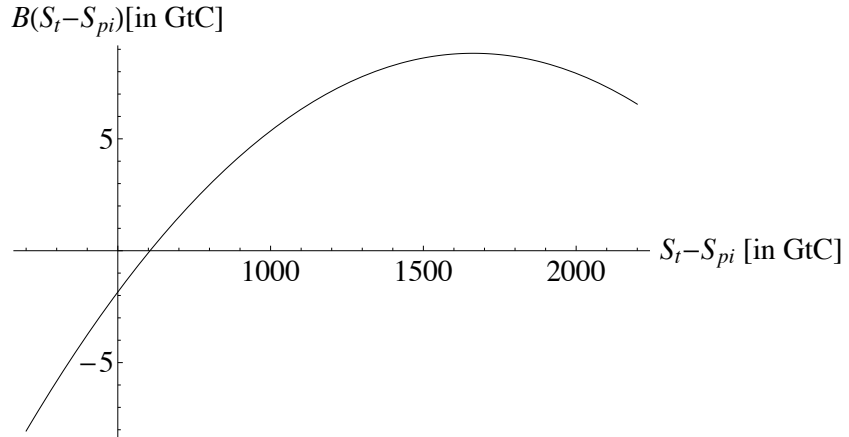


Figure 7: Fitted absolute decay rate $B(S_t - S_{pi})$ in GtC for any given atmospheric stock change level ($S_t - S_{pi}$) for CJL

The concave function as in figure 7 suggests the form of an inverted-U-shaped function put forward in literature.³⁵

³⁴It is evident that a linearly fitted relative rate function of the form $a - b \cdot x$ implies a parabolic (i.e., polynomial) function of the form $a \cdot x - b \cdot x^2$, which looks downwards, if multiplied with x . Be aware of the negative axis intercept of the polynomial function. Thus, one could not derive a reasonable relative decay rate back from it.

³⁵Note that the simple $B(S_t)$ -function (for CJL) would have also shown the inverted U-shape.

3.3 Functional decay forms

In order to be to real circumstances as near as possible, the rate of decay (or alternatively, the net carbon sink flow rate) can be modeled as an inverted-U shaped curve [e.g., Forster, 1975; Cesar and de Zeeuw, 1994; Clark and Reed, 1994; Tahvonen and Withagen, 1996; Tahvonen and Salo, 1996; Toman and Withagen, 2000; Prieur, 2008] (similar to the environmental Kuznets curve)³⁶, and can have multiple steady states and multiple trajectories [Forster, 1975; Tahvonen and Salo, 1996].³⁷ An inverted U-shaped decay curve sheds light upon the bounded natural capacity of pollution assimilation.

The geneneral modelling of the inverted U-function of pollution accumulation is given as an absolute rate $B(S_t)$. It is important to distinguish between the absolute and the relative rate $\beta(S_t)$ where

$$B(S_t) = \beta(S_t) \cdot S_t \quad (4)$$

Both decay rates are measured as stock removals per time unit.³⁸ If absolute $B(S_t)$ is concavely growing, then relative $\beta(S_t)$ is convexly falling because the removal percentage sinks with a higher S_t (i.e., the airborne fraction rises). Forster [1975] names $\beta(S_t)$ the non-constant exponential decay rate when $B(S_t)$ shows

³⁶I.e., this same result is seen in the behavior of the environmental Kuznets curve (EKC) [Kuznets, 1955], which follows some pollutant variable (e.g., level of CO₂ emissions) as an inverted U-function of the per capita income variable [Yandle et al., 2002]. An environmental decay is observed until the turning point of this same function is reached, and afterwards an environmental improvement progresses with the income variable (until atmospheric CO₂ levels abate to the pre-industrial ones), suggesting the development path to be described by both environmental quality improvements and economic growth [Antle and Heidebrink, 1995]. This means that in the short run an abatement method can decrease the magnitude of mitigation, whilst in the long run it can increase it.

³⁷Nowadays it is farfetched to assume the nature's uptake capacity to imply a constant (average) decay rate β instead of $\beta(S_t)$ or $\beta(S_t - S_{pi})$, thus a proportionately or linearly rising $B(S_t)$ (i.e., $B(S_t - S_{pi}) = \beta \cdot (S_t - S_{pi})$ or $B(S_t) = \beta \cdot (S_t)$) where the modelling of the natural uptake sinks are not seen to be dependent on positive carbon cycle feedbacks and the accumulated stock, as it sometimes was put forward in past literature [e.g., d'Arge, 1971; Keeler et al., 1971; Plourde, 1972; Forster, 1973; Van der Ploeg and Withagen, 1991; Smulders and Gradus 1993, John and Pecchenino, 1994].

³⁸The absolute decay (rate) function $B(S_t)$ specifies the level of pollution absorbed by nature in every period, whereas the relative decay (rate) function $\beta(S_t)$ gives the percentage of pollution absorbed by nature in every period. It resembles something like the opposite of the airborne fraction (i.e., $(1 - a) = \beta$).

a concave function as the inverted-U shape. $B(S_t)$ implies a twice continuously differentiable function $B(S_t): R_+ \rightarrow R_+$ satisfying $B(0) = 0$, $B(S_t) > 0 \forall 0 < S_t < \bar{S}_t$, $B(S_t) = 0 \forall S_t \geq \bar{S}_t > 0$. The latter emphasizes that the decay rate becomes zero after a critical high stock pollution level \bar{S}_t [e.g., Strøm, 1972] where natural decay becomes irreversible, or accordingly, where nature's regeneration ability changes irreversibly (e.g., from a net carbon sink into a net carbon source). Forster [1975, p. 2] stresses that below \bar{S}_t "the pollution has destroyed the natural clean-up processes in the environment". $B(S_t)$ can be divided into a reversible and an irreversible region. In the reversible area the decay rate behaves strictly concave and in the irreversible area the decay rate is equal to zero [e.g., Tahvonen and Withagen, 1996]. Furthermore, it holds that $\frac{\partial^2 B}{\partial^2 S_t} < 0 \forall 0 < S_t < \bar{S}_t$ with $\frac{\partial B}{\partial S_t} > 0 \forall 0 < S_t \leq S_{t*}$ and $\frac{\partial B}{\partial S_t} < 0 \forall S_{t*} < S_t < \bar{S}_t$ where $\frac{\partial B}{\partial S_t} = 0$ for S_{t*} . Problems may arise after the critical irreversible point \bar{S}_t in terms of non-differentiability. Also, nonconvexities in dynamic optimization should be assumed, even if they cause problems in calculating the right solutions. Another specification of the absolute decay rate function could be a convexly falling curve after the saturation point (i.e., turning point). That is, the decay function concavely rises when stock pollution is low, and below S_{t*} convexly falls when the latter is high [Tahvonen and Salo, 1996] with $\frac{\partial^2 B}{\partial^2 S_t} < 0 \forall 0 < S_t \leq S_{t*}$ and $\frac{\partial^2 B}{\partial^2 S_t} > 0 \forall S_{t*} < S_t < \bar{S}_t$. This allows a more pessimistic scenario.³⁹ Other modifications from the inverted U-function are also possible [e.g., Toman and Withagen, 1998].

What comes out as a result are two possibilities for an optimal control policy. First, for the irreversible state the adequate policy should incorporate zero carbon emissions when the stock pollution level is high. Second, for the reversible state the appropriate policy can afford to maintain positive carbon emissions, even if the level of carbon pollution should stay positively low in order to allow the decay rate to be increasing [Tahvonen and Withagen, 1996]. Looking at today's situation, we should stop consuming scarce resources and enable environmentally

³⁹The most drastic scenario would probably be a concave growth function until S_{t*} as a fixed ceiling of saturation and therefore a non-continuous jump to a decay rate of zero.

friendly, efficient resource allocations instead. The stabilization (at the atmospheric CO₂ level of ~ 450 ppm) remains as the most important task in order to control climate change. This can mainly be achieved by a drastic curbing of the worldwide emissions [e.g., Le Quéré et al., 2009; IPCC, 2007].⁴⁰

4 The model

We assume a model where the social planner authorities seek to maximize the following intertemporal discounted welfare function

$$\max_{C(t)>0, 0\leq m(t)\leq 1} E \int_0^\infty e^{-\rho t} [U(C(t))] dt \quad (5)$$

subject to the following constraints

$$\frac{dS}{dt} = (\epsilon \cdot Y(K) \cdot (1 - m) - B(S - S_{pi})) \quad (6)$$

$$B(S - S_{pi}) = \beta(S - S_{pi}) \cdot (S - S_{pi}) \quad (7)$$

$$\frac{Y(K)}{D(T(S))} = I + C + M(m, Y(K)) \quad (8)$$

$$\frac{dK}{dt} = (I - \delta \cdot K) \quad (9)$$

$$S(0) = S_0, K(0) = K_0 \quad (10)$$

This model corresponds to the one of Lontzek and Narita [2011]. The integral

⁴⁰Unfortunately, global emissions continue to rise and are not likely to fall in the near future. While fossil fuel combustion keeps increasing, emissions due to land-use-change have stayed more or less constant over time [e.g., Le Quéré et al., 2009; Canadell et al., 2007]. Therefore, a deep cut in global emissions is virtually impossible.

(5) is to be maximized subject to the constraints (6) - (10). With the first state transitional differential function (6) we see how the carbon stock in the atmosphere S changes through time. We assume an economy where the gross output Y is dependent on the capital stock K , and where it holds $\frac{\partial Y}{\partial K} > 0$ and $\frac{\partial^2 Y}{\partial^2 K} < 0$. The proportion ϵ indicates the polluting coefficient of Y (i.e., how much of the emissions have an impact on the environment). Mitigation m describes the proportion under control, thus only $(1 - m)$ is released to the atmosphere. $\epsilon \cdot Y(K) \cdot (1 - m)$ defines the atmospheric accumulation of emissions. The decay function is captured by $B(S - S_{pi})$ (7) and denotes the atmospheric decay of the carbon into the oceanic and terrestrial sinks. Note from (7) that $B(S - S_{pi})$ incorporates a decay rate β which is dependent on the carbon atmospheric stock change since the preindustrial level S_{pi} .⁴¹ The decay function comes from the previous chapter where we derived the respective *beta*-functions (i.e., linearly fitted forms). By multiplying it with $(S - S_{pi})$ we obtain the concave function $B(S - S_{pi})$.⁴² An increase in atmospheric carbon stocks causes an increase in mean global temperature and thus the temperature function is given by $T(S)$ with properties $\frac{\partial T}{\partial S} > 0$ and $\frac{\partial^2 T}{\partial^2 S} < 0$. An increased temperature, in turn, has an impact on Y with a damage function $D(T)$ implying $\frac{\partial D}{\partial T} > 0$, $\frac{\partial^2 D}{\partial^2 T} < 0$ and $D(0) = 1$. Equation (8) represents the output balance condition. The quotient on the left-hand side is the net output (i.e., gross output less output damage).⁴³ The right-hand-side is the sum of investment I , consumption C and the costs of mitigation $M(m, Y(K))$ ⁴⁴ with properties $\frac{\partial M}{\partial m} > 0$, $\frac{\partial^2 M}{\partial^2 m} > 0$, $\frac{\partial M}{\partial Y} > 0$, $\frac{\partial^2 M}{\partial^2 Y} = 0$ and $\frac{\partial^2 M}{\partial Y \partial m} = \frac{\partial^2 M}{\partial m \partial Y} > 0$. The second state transitional differential function (9) denotes how the capital stock evolves through time. The rate of capital depreciation is indicated by $1 \geq \delta \geq 0$. The atmospheric stock of carbon and the capital stock at $t = 0$ equal S_0 and K_0 (10).

⁴¹Throughout, we specify this level to be 285 ppm, that is 605.34 GtC, for the decay functions.

⁴²The properties for $B(S - S_{pi})$ are discussed in chapter 3.3.

⁴³The variable S in the damage function D should actually be $(S - S_{pi})$. However, this is captured by the corresponding functional form later.

⁴⁴I.e., the abatement spenditure. It is a function of the mitigation proportion m and the gross output $Y(K)$.

The control variables⁴⁵ are consumption C ⁴⁶ and mitigation m , and the aim is to find their dynamically optimal choice. The optimal choice of investment I can afterwards be derived directly by constraints (8) - (9). We maximize the expected present welfare of utility and incorporate a utility function with constant relative risk aversion.⁴⁷ For $U(C)$ it holds that $\frac{\partial U}{\partial C} > 0$ $\frac{\partial^2 U}{\partial^2 C} < 0$ and therefore we assume a strictly concave, risk averse, utility function of current consumption. ρ reads the rate of time preferencing (i.e., continuous time discounting) and is ≥ 0 .⁴⁸ The state variables describing the system's state at any given time are the atmospheric carbon stock S and the capital stock K .⁴⁹

The optimization problem is solved deterministically. We do not assume uncertainty or stochastic processes in the climate change. We are aware of the fact that this is a rather limiting assumption. The problem's type is of continuous time rather than discrete time.⁵⁰ The time horizon is assumed to be infinite.⁵¹ What we mainly pursue to find are the optimal paths for the control variables (e.g., $(C(t)^*)_{t=0}^{\infty}$) and the state variables (e.g., $(S(t)^*)_{t=0}^{\infty}$).

The following is solved for the general form of the model. Thus it can be

⁴⁵They are characterized by a flow.

⁴⁶I.e., the choice variable which is integrated in the utility function.

⁴⁷As the specific functional forms of the dynamic optimization problem are given afterwards, it is nonetheless worthy to state that CRRA is characterized by $U(C) = \frac{C^{1-\alpha}}{1-\alpha}$ for $\alpha > 0$, $\alpha \neq 1$, and $U(C) = \ln(C)$ for $\alpha = 1$. In this case the value of α is constant (i.e., it can be checked by the Arrow-Pratt definition) and thus denotes the coefficient of relative risk aversion, whilst the quotient $\frac{1}{\alpha}$ indicates the intertemporal substitution elasticity of consumption [Jehle and Reny, 2011].

⁴⁸The discount factor γ equals $\frac{1}{1+\rho}$. Non-discounting would invoke $\gamma = 1$ or $\rho = 0$. Maximal discounting, on the other hand, would invoke $\gamma = 0$ or $\rho \rightarrow \infty$. Therefore ρ is ≥ 0 .

⁴⁹They are characterized by a stock.

⁵⁰If continuous, time is treated as a continuum with differential equations instead of difference equations for the state variables, and the maximization problem stated as the integral of the flow of continuous utilities instead of the sum of discrete ones.

⁵¹Note that there exist three major differences: infinite vs. finite, continuous vs. discrete, deterministic vs. stochastic.

replaced by any functional form later.⁵² The current value Hamiltonian reads:⁵³

$$\begin{aligned}\mathcal{H} = & U(C) \\ & + \lambda_S (\epsilon Y(K)(1 - m) - B(S - S_{pi})) \\ & + \lambda_K \left(\frac{Y(K)}{D(T(S))} - C - M(m, Y(K)) - \delta K \right)\end{aligned}\quad (11)$$

The first-order conditions of the Pontryagin maximum principle are determined by

$$\begin{aligned}\mathcal{H}'(C) & \stackrel{!}{=} 0 \Rightarrow \\ U'(C) & = \lambda_K\end{aligned}\quad (12)$$

$$\begin{aligned}\mathcal{H}'(m) & \stackrel{!}{=} 0 \Rightarrow \\ M'(m, Y(K)) & = -\frac{\lambda_S \epsilon Y(K)}{\lambda_K}\end{aligned}\quad (13)$$

$$\begin{aligned}\mathcal{H}'(S) & \stackrel{!}{=} -(\dot{\lambda}_S - \rho \lambda_S) \Rightarrow \\ B'(S - S_{pi}) \lambda_S & + \frac{\lambda_K Y(K)}{[D(T(S))]^2} D'(T(S)) T'(S) = \dot{\lambda}_S - \rho \lambda_S\end{aligned}\quad (14)$$

$$\begin{aligned}\mathcal{H}'(K) & \stackrel{!}{=} -(\dot{\lambda}_K - \rho \lambda_K) \Rightarrow \\ \lambda_K \left(\frac{Y'(K)}{D(T(S))} - M'(m, Y(K)) Y'(K) - \delta \right) & \\ + \lambda_S \epsilon Y'(K)(1 - m) & = \rho \lambda_K - \dot{\lambda}_K\end{aligned}\quad (15)$$

λ_S and λ_K indicate the shadow prices of S and K , respectively. They define the change in the objective function (i.e., the marginal benefit when relaxing one constraint, or the marginal cost when strenghtening one constraint). The

⁵² $B(S - S_{pi})$ is taken (without any reason) instead of its specific form (equation (7)).

⁵³The current Hamiltonian (from optimal control theory) is derived from $\mathcal{H}(C, m, S(t), K(t)) = U(C, m, S(t), K(t)) + \lambda(t)\theta(C, m, S(t), K(t))$ with $\theta(C, m, S(t), K(t))$ equal to \dot{S} or \dot{K} . Note that we could have also applied the continuous Bellman equation (from dynamic programming) $(\rho V(S(t), K(t)) = \max_{C(t) \geq 0, 0 \leq m(t) \leq 1} U(C, m, S(t), K(t)) + V'(S(t), K(t))\theta(C, m, S(t), K(t))$ for this case, where $V(S(t), K(t))$ would have been the value function to be found and $V'(S(t), K(t))$ the shadow prices (i.e., the opportunity costs of the alternative) of S and K . The two approaches are equal if $\lambda_t \equiv V'(S(t), K(t))$. Notice that we dropped the subscript t in the following.

transversality conditions are given by

$$\lim_{t \rightarrow \infty} \lambda_S e^{-\rho t} S = 0, \quad \lim_{t \rightarrow \infty} \lambda_K e^{-\rho t} K = 0 \quad (16)$$

Now we analyze the steady states and their general properties. From the first-order conditions of the control variables (12) - (13) we obtain $C \equiv C(\lambda_K)$ and $m \equiv m(K, \lambda_S, \lambda_K)$ with $\frac{\partial C}{\partial \lambda_K} < 0$, $\frac{\partial m}{\partial K} > 0$, $\frac{\partial m}{\partial \lambda_S} > 0$ and $\frac{\partial m}{\partial \lambda_K} < 0$.⁵⁴ The modified Hamiltonian dynamic system, shortly MHDS, is deduced from the equations of motion for the state variables and the first-order conditions of the co-state variables. It reads⁵⁵

$$\dot{S} = \epsilon Y(K)(1 - m(K, \lambda_S, \lambda_K)) - B(S - S_{pi}) \quad (17)$$

$$\dot{K} = \frac{Y(K)}{D(T(S))} - C(\lambda_K) - M(m(K, \lambda_S, \lambda_K), Y(K)) - \delta K \quad (18)$$

$$\dot{\lambda}_S = \lambda_S(B'(S - S_{pi}) + \rho) + \frac{\lambda_K Y(K)}{[D(T(S))]^2} D'(T(S)) T'(S) \quad (19)$$

$$\begin{aligned} \dot{\lambda}_K &= \lambda_K \left(\rho - \frac{Y'(K)}{D(T(S))} + M'(m(K, \lambda_S, \lambda_K), Y(K)) Y'(K) + \delta \right) \\ &\quad - \lambda_S \epsilon Y'(K)(1 - m(K, \lambda_S, \lambda_K)) \end{aligned} \quad (20)$$

The steady-state analysis inquires $\dot{S} = \dot{K} = \dot{\lambda}_S = \dot{\lambda}_K = 0$ and therefore for the equations of MHDS (17) - (20):

$$C(\lambda_K) = \frac{Y(K)}{D(T(S))} - M(m(K, \lambda_S, \lambda_K), Y(K)) - \delta K \quad (21)$$

$$m(K, \lambda_S, \lambda_K) = 1 - \epsilon Y(K) B(S - S_{pi}) \quad (22)$$

$$\lambda_S = \frac{-\lambda_K Y(K) D'(T(S)) T'(S)}{(B'(S - S_{pi}) + \rho) [D(T(S))]^2} \quad (23)$$

$$\lambda_K = \frac{\lambda_S \epsilon Y'(K)(1 - m(K, \lambda_S, \lambda_K))}{\rho - \frac{Y'(K)}{D(T(S))} + M'(m(K, \lambda_S, \lambda_K), Y(K)) Y'(K) + \delta} \quad (24)$$

The Jacobian matrix of the MHDS in the steady state is determined by (25).

⁵⁴Note that the control variables C and m are explicitly given with the inverse function by $F_U^{-1}(\lambda_K)$ and $F_M^{-1}(\frac{-\lambda_S \epsilon Y(K)}{\lambda_K})$ respectively.

⁵⁵Notice that these are the partial derivatives s.t. time (e.g., $\frac{dS}{dt} = \dot{S} = S'(t)$).

$$J = \begin{bmatrix} \frac{\partial \dot{S}}{\partial S} & \frac{\partial \dot{S}}{\partial K} & \frac{\partial \dot{S}}{\partial \lambda_S} & \frac{\partial \dot{S}}{\partial \lambda_K} \\ \frac{\partial \dot{K}}{\partial S} & \frac{\partial \dot{K}}{\partial K} & \frac{\partial \dot{K}}{\partial \lambda_S} & \frac{\partial \dot{K}}{\partial \lambda_K} \\ \frac{\partial \dot{\lambda_S}}{\partial S} & \frac{\partial \dot{\lambda_S}}{\partial K} & \frac{\partial \dot{\lambda_S}}{\partial \lambda_S} & \frac{\partial \dot{\lambda_S}}{\partial \lambda_K} \\ \frac{\partial \dot{\lambda_K}}{\partial S} & \frac{\partial \dot{\lambda_K}}{\partial K} & \frac{\partial \dot{\lambda_K}}{\partial \lambda_S} & \frac{\partial \dot{\lambda_K}}{\partial \lambda_K} \end{bmatrix} \quad (25)$$

where

$$\begin{aligned} \frac{\partial \dot{S}}{\partial S} &= -B'(S - S_{pi}) \\ \frac{\partial \dot{S}}{\partial K} &= \epsilon Y'(K)(1 - m(K, \lambda_S, \lambda_K)) - \epsilon Y m'(K) \\ \frac{\partial \dot{S}}{\partial \lambda_S} &= -\epsilon Y(K) m'(\lambda_S) \\ \frac{\partial \dot{S}}{\partial \lambda_K} &= -\epsilon Y(K) m'(\lambda_K) \\ \frac{\partial \dot{K}}{\partial S} &= \frac{-Y(K)}{[D(T(S))]^2} D'(T(S)) T'(S) \\ \frac{\partial \dot{K}}{\partial K} &= \frac{Y'(K)}{D(T(S))} - M'(m(K, \lambda_S, \lambda_K), Y(K)) m'(K) Y'(K) - \delta \\ \frac{\partial \dot{K}}{\partial \lambda_S} &= -M'(m(K, \lambda_K, \lambda_S), Y(K)) m'(\lambda_S) \\ \frac{\partial \dot{K}}{\partial \lambda_K} &= -M'(m(K, \lambda_K, \lambda_S), Y(K)) m'(\lambda_K) - C'(\lambda_K) \\ \frac{\partial \dot{\lambda_S}}{\partial S} &= \lambda_S B''(S - S_{pi}) - \frac{\lambda_K Y(K)}{[D(T(S))]^3} D'(T(S)) T'(S) D'(T(S)) T'(S) \\ &\quad + \frac{\lambda_K Y(K)}{[D(T(S))]^2} D''(T(S)) T'(S) T'(S) + \frac{\lambda_K Y(K)}{[D(T(S))]^2} D'(T(S)) T''(S) \\ \frac{\partial \dot{\lambda_S}}{\partial K} &= \frac{\lambda_K Y'(K)}{[D(T(S))]^2} D'(T(S)) T'(S) r \\ \frac{\partial \dot{\lambda_S}}{\partial \lambda_S} &= B'(S - S_{pi}) + \rho \\ \frac{\partial \dot{\lambda_S}}{\partial \lambda_K} &= \frac{Y(K) D'(T(S)) T'(S)}{[D(T(S))]^2} \\ \frac{\partial \dot{\lambda_K}}{\partial S} &= \frac{\lambda_K Y'(K)}{[D(T(S))]^2} D'(T(S)) T'(S) \\ \frac{\partial \dot{\lambda_K}}{\partial K} &= \frac{-\lambda_K Y''(K)}{D(T(S))} + \lambda_K M''(m(K, \lambda_S, \lambda_K), Y(K)) Y'(K) m'(K) Y'(K) \\ &\quad + \lambda_K M'(m(K, \lambda_S, \lambda_K), Y(K)) Y''(K) - \lambda_S \epsilon Y''(K)(1 - m(K, \lambda_S, \lambda_K)) \\ &\quad + \lambda_S \epsilon Y'(K) m'(K) \\ \frac{\partial \dot{\lambda_K}}{\partial \lambda_S} &= \lambda_K M'(m(K, \lambda_S, \lambda_K), Y(K)) m'(\lambda_S) Y'(K) \\ &\quad - \epsilon Y'(K)(1 - m(K, \lambda_K, \lambda_S)) + \lambda_S \epsilon Y'(K) m'(\lambda_S) \\ \frac{\partial \dot{\lambda_K}}{\partial \lambda_K} &= \rho - \frac{Y'(K)}{D(T(S))} + M'(m(K, \lambda_S, \lambda_K), Y(K)) Y'(K) + \delta \\ &\quad + \lambda_K M''(m(K, \lambda_S, \lambda_K), Y(K)) m'(\lambda_K) Y'(K) \\ &\quad + \lambda_S \epsilon Y'(K) m'(\lambda_K) \end{aligned}$$

From the Jacobian matrix J (25) we can calculate its eigenvalues. They result from $|J - I \cdot z| = 0$ where I defines the identity matrix. They are stated as $\{z_1, z_2, z_3, z_4\}$ where z_2 and z_4 are the negative eigenvalues in the system. The values for the steady states are given by S_{SS} , K_{SS} , λ_{SSS} and λ_{KSS} (i.e., A_{SS}).⁵⁶ The optimal time paths A_t^* for $S(t)$, $K(t)$, $\lambda_S(t)$ and $\lambda_K(t)$ can be obtained with the following equation:

$$A_t^* = A_{SS} + e^{z_2 t} B_2 C_{A,z_2} + e^{z_4 t} B_4 C_{A,z_4} \quad \forall A \in S, K, \lambda_S, \lambda_K \text{ and } i \in 2, 4 \quad (26)$$

where $C_{zi,A}$ is the eigenvector referred to the negative eigenvalue i [e.g., Lontzek, 2011]. B_i are arbitrary boundaries of integration for the optimal initial state variables S and K . They are indicated by $A_0^* = A_0$.⁵⁷

5 Results

For the problem stated in section 4 the functional forms are given by $Y(K) = L \cdot K^\nu$, $D(T(S)) = 1 + \kappa \cdot T(S)^2$, $T(S) = \tau \cdot (S - S_{PI})$, $M(m, Y(K)) = \psi \cdot \epsilon \cdot Y(K) \cdot m^2$ and $U(C) = \frac{C^{1-\alpha}}{1-\alpha}$.⁵⁸ Additionally, the corresponding parameter values are given by:⁵⁹ $L = 1$, $\alpha = 0.5$, $S_{PI} = 400^{60}$, $\delta = 0.1$, $\epsilon = 0.1$, $\kappa = 0.005$, $\nu = 0.75$, $\tau = 0.003$, $\rho = 0.01$ and $\psi = 2$.

⁵⁶As the optimization problem for the deterministic case was set up with the state - costate system for the states atmospheric carbon stock and capital and their respective shadow prices rather than with the Ramsey-Keynes rule for optimal consumption (and mitigation), the steady states of the latter have to be solved by plugging the obtained steady states values into the constraints or the first-order conditions. The same can be done for the optimal investments.

⁵⁷They are either 800 for S or 500 for K .

⁵⁸Some explaining remarks: κ is the economic variable and expresses $T(S)$ in economic units. $M(m, Y(K))$ has to incorporate some quadratic form (e.g., m^2) as it refers to a quadratic cost function. τ is the temperature. ν defines how many tons of CO₂ one unit of GDP fabricates. ψ is the cost parameter and transforms tons of CO₂ into units of money.

⁵⁹Again, the functions and parameters are consistent with the ones used in Lontzek and Narita [2011]. Consult the authors for the motives of the chosen values.

⁶⁰Note the difference between S_{pi} and S_{PI} . Thus, the parameter is not the same for the decay function as for the damage or the temperature function.

The results are given for SRES and CJL. The functional forms of *beta* were derived in subchapter 3.2. Because of nonlinear functions and the multidimensionality, a numerical analysis is inevitable. In the next two subchapters, the results for SRES and CJL are presented. The results for all relevant variables, especially for mitigation, are thoroughly discussed for SRES. Since the results for CJL show a similar pattern as the ones for SRES, CJL is not discussed as carefully.

5.1 SRES projections

Figure 8 plots the optimal time paths for the state variables and their shadow prices. It also shows the time paths for the direct control variable C and the indirect control variable I^{61} . Atmospheric stock of carbon is given in GtC. Consumption, investment, capital stock and mitigation costs, which are presented later, are given in units of output. The shadow prices are dimensionless, they define rates per time unit. Numerical computation leads to the following steady states - for B1: $S_{SS} = 1072.19$, $K_{SS} = 896.926$, $\lambda_{SSS} = -0.353$, $\lambda_{KSS} = 0.133$; for A1B: $S_{SS} = 1252.37$, $K_{SS} = 952.665$, $\lambda_{SSS} = -0.264$, $\lambda_{KSS} = 0.127$; for A1FI: $S_{SS} = 1460.69$, $K_{SS} = 1011.57$, $\lambda_{SSS} = -0.193$, $\lambda_{KSS} = 0.125$. Note that the results are reasonable (e.g., A1FI (worst case) displays the highest S levels over time, whereas B1 (best case) shows the lowest ones which is due to their different emission scenarios). Keep in mind the Pontryagin first-order conditions. Equation (12) states that marginal utility from consumption is equal to the shadow price of capital. For (13) it holds that λ_S^{62} must be ≤ 0 . This can be seen in figure 8. Because temperature $T(S)$ rises proportionately with higher atmospheric carbon concentration S , λ_S declines with higher S . In addition, for λ_K it holds ≥ 0 , and thus the shadow price of K declines with higher K (i.e., $\frac{\partial K}{\partial \lambda_K} < 0$ if λ_K rises

⁶¹Investment is not a direct control variable as it does not occur in the set up of the optimization problem. However, it is an economically interesting variable as it can be derived from the direct variables.

⁶²We could also write λ_S^* to refer to the optimal time path. The same notation with an asterisk is valid when examining other variables.

by one unit). However, this condition only holds until $t \approx 40$. Throughout we can observe that C rises if K rises (i.e., $\frac{\partial C}{\partial K} > 0$). The same conforms to the investments (i.e., $\frac{\partial I}{\partial K} > 0$). Larger capital stocks invoke larger levels of investment.⁶³ Intuitively appealing is the effect on the dynamically optimal mitigation policy m^* ⁶⁴: If K is held fixed, then $\frac{\partial m^*}{\partial S} > 0$. However, if we look at figure 9, which shows the optimal path of m , we notice a strange pattern.⁶⁵ Even if A1FI depicts the largest S , the mitigation policy accounts for only 30% in the steady state, whereas B1 accounts for a percentage twice as large. The counterintuitive patterns of m are hard to explain. It suggests a very pessimistic world, where the optimal mitigation moves on a higher level when the slope of the optimal atmospheric stock curve is flatter (look at B1). The same pattern can be observed with the shadow price of carbon. For B1 λ_S is more negative than for A1FI. This should not be the case as the social costs of carbon⁶⁶ for A1FI should be larger than for B1.

Net Output characterized by the gross output less damage (i.e., $\frac{Y(K)}{D(T(S))}$) is to be allocated between C , I and $M(m)$ ⁶⁷. The same concept of allocations is applied in Lontzek and Narita [2011]. We write the allocations as ξ_i ⁶⁸ for $i \in C, M(m), I$, where $\xi_C + \xi_{M(m)} + \xi_I$ adds up to 1. If we hold $\xi_{M(m)}$ fixed, then a higher ξ_I will result in a lower ξ_C . These effects are shown in figure 10 and 11. Notice the symmetry in figure 11. We can derive this assumption easily from figure 10 as $\xi_{M(m)}$ is nearly 0, it ranges from 0 - 0.6%. Such a low percentage for investment into abatement is again quite surprising. On the other hand, if we hypothetically held ξ_C fixed, then $\xi_{M(m)}$ and ξ_I had to be weighed against each other. Following the thoughts of Lontzek and Narita [2011], the trade-off is between low climate damage (from abatement) versus high capital returns

⁶³I.e., whether capital accumulation is high is a question of investment.

⁶⁴Here we use the asterisk for emphasis.

⁶⁵The same observation applies to figure 10 later.

⁶⁶That is the price of the environmental damage caused by one marginal ton of CO₂ released into the atmosphere.

⁶⁷Note here that we use $M(m) = \psi \cdot m(t)^2$ rather than $M(m, Y(K)) = \psi \cdot \epsilon \cdot L \cdot K(t)^\nu \cdot m(t)^2$.

⁶⁸I.e., $\xi_C \cdot \frac{Y(K)}{D(T(S))} = C$, $\xi_I \cdot \frac{Y(K)}{D(T(S))} = I$, $\xi_{M(m)} \cdot \frac{Y(K)}{D(T(S))} = M(m)$. Note again, I is calculated with $M(m)$ rather than $M(m, Y(K))$.

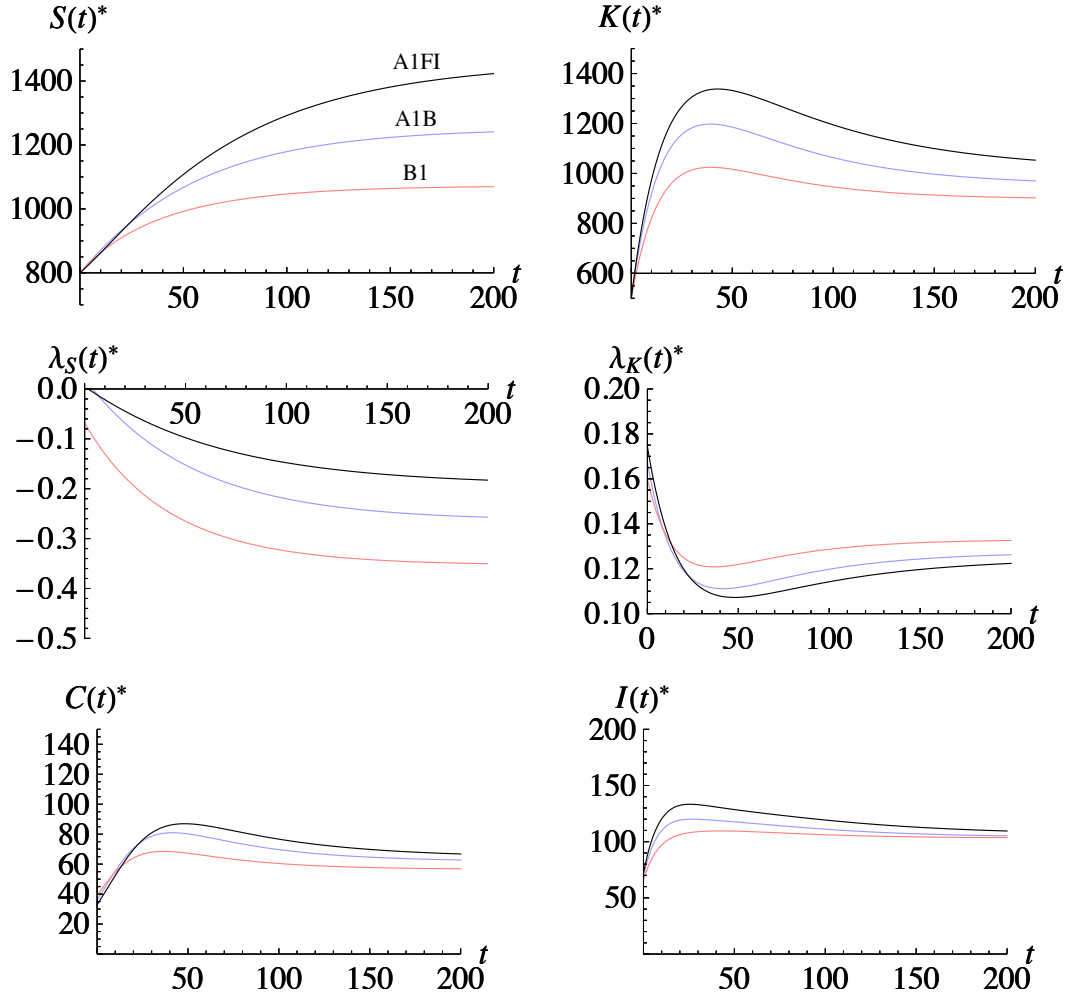


Figure 8: Optimal time paths $A_t^* \forall A \in S, K, \lambda_S, \lambda_K, C, I$ for any given time t for SRES. S is given in GtC; K, C, I are given in units of output; λ_S, λ_K are dimensionless. The coloured curves help to distinguish between B1, A1B and A1FI.

(from investment). Furthermore, ξ_C and $\xi_{M(m)}$ project a similar trajectory. Both variables rise with higher S . The steady state allocations for $M(m)$ range between 0.1 - 0.55%. Note that the corresponding S_{SS} is high, whilst K_{SS} is rather low. ξ_C in the steady state is $\approx 40\%$, whereas ξ_I is $\approx 60\%$.

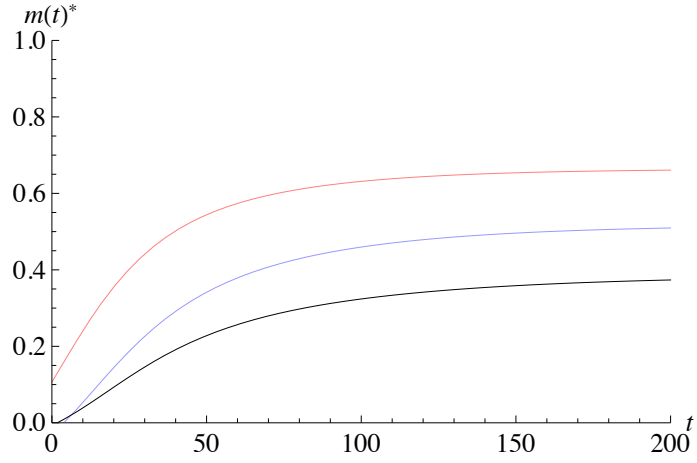


Figure 9: Optimal mitigation m_t^* as a decimal number (ratio) for any given time t for SRES

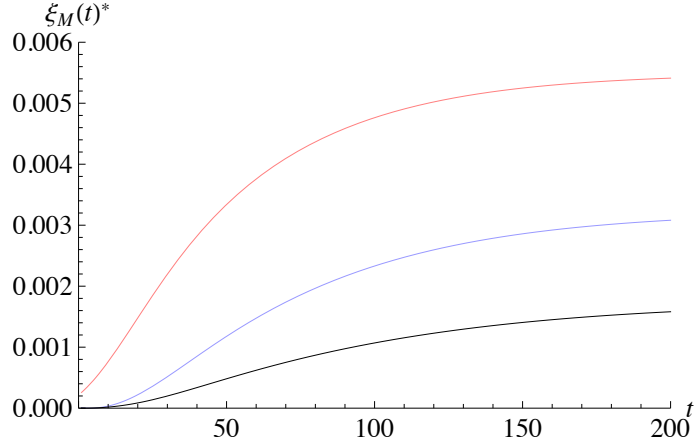


Figure 10: Optimal allocation $\xi_{M(m)}(t)^*$ as a decimal number (ratio) for any given time t for SRES

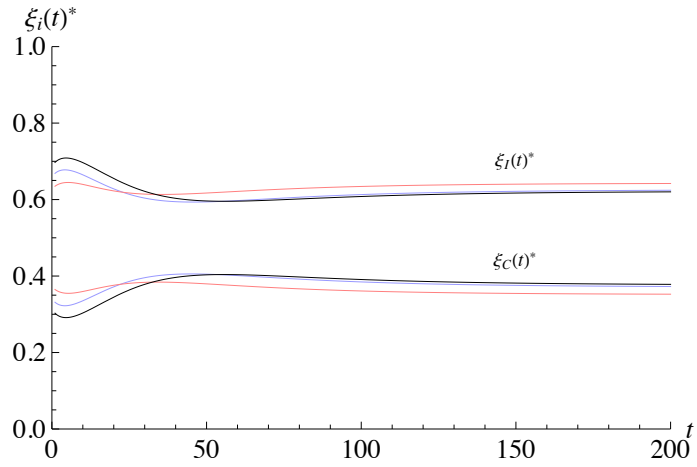


Figure 11: Optimal allocations $\xi_C(t)^*$ and $\xi_I(t)^*$ as a decimal number (ratio) for any given time t for SRES

5.2 CJL projection

Results from CJL exhibit the same patterns as SRES. Therefore, we will not discuss them in detail. However, one feature stands out. The steady state level of the carbon stock is very high. It is even much higher than S_{SS} for A1FI. Nature would most certainly collapse if CJL was going to happen.⁶⁹ All other variables range in similar intervals like in SRES.

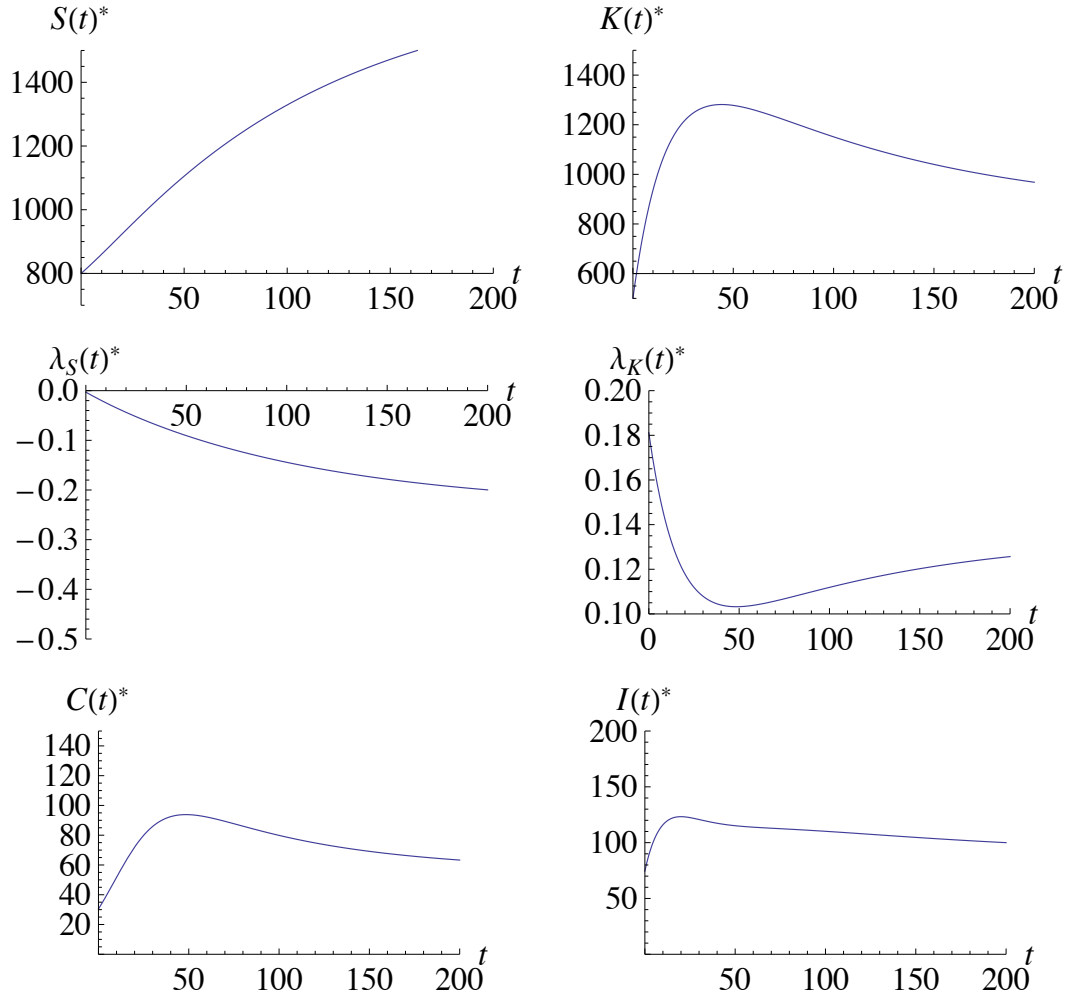


Figure 12: Optimal time paths $A_t^* \forall A \in S, K, \lambda_S, \lambda_K, C, I$ for any given time t for CJL. S is given in GtC; K, C, I are given in units of output; λ_S, λ_K are dimensionless.

⁶⁹Nature would also collapse if A1FI was going to happen. Keep the stabilization target range from 450 ppm (956 GtC) - 550 ppm (1168 GtC) in mind. Only B1's steady state of S ranges in this interval. Though, we have to consider the large time period $t = 200$, which makes things more uncertain.

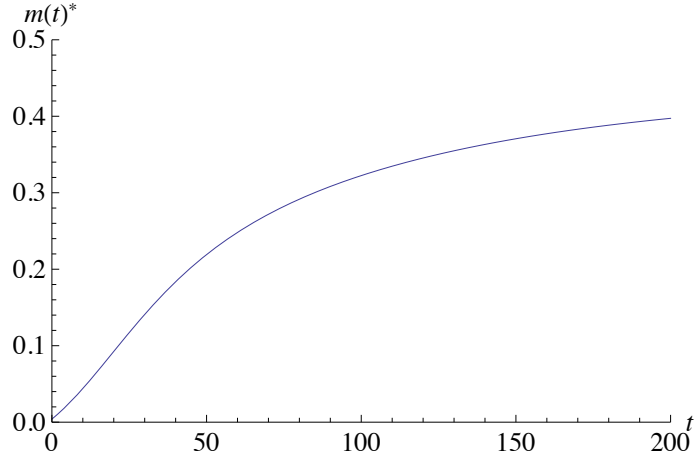


Figure 13: Optimal mitigation m_t^* as a decimal number (ratio) for any given time t for CJL

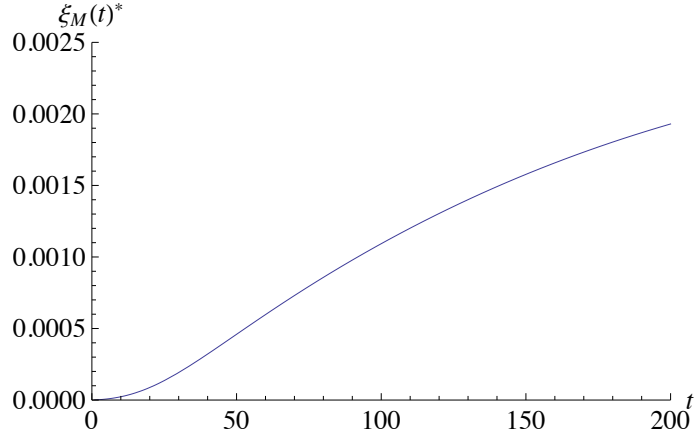


Figure 14: Optimal allocation $\xi_{M(m)}(t)^*$ as a decimal number (ratio) for any given time t for CJL

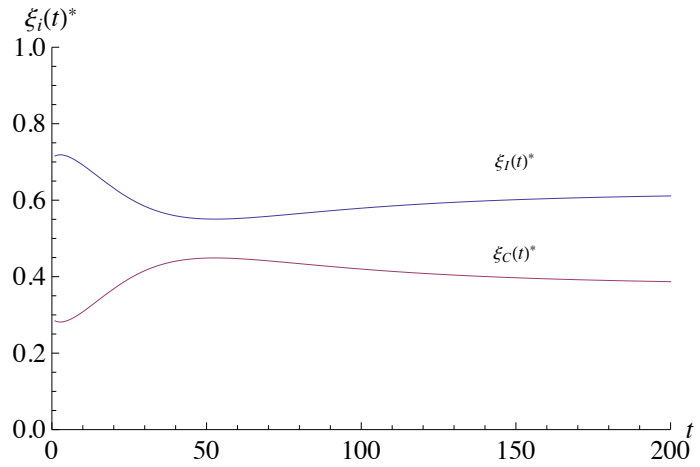


Figure 15: Optimal allocations $\xi_C(t)^*$ and $\xi_I(t)^*$ as a decimal number (ratio) for any given time t for CJL

The deterministic steady states for CJL are given by $S_{SS} = 1718.84$, $K_{SS} = 844.035$, $\lambda_{SSS} = -0.237$, $\lambda_{KSS} = 0.135$ and are displayed in figure 12. Figure 13 maps the optimal mitigation policy for CJL and m_t^* is $\approx 40\%$. That is not as bad compared to A1FI. The steady state for $\xi_{M(m)}$ still seems to rise behind $t = 200$ (i.e., figure 14). However, it is not suggested to pass the benchmark of 0.25% and thus behaves as $\xi_{M(m)}$ for A1FI. Finally, figure 15 presents the ξ_I and ξ_C . The respective steady states are the same as in SRES due to the low $\xi_{M(m)}$.

6 Conclusion

The global carbon cycle incorporates noticeable vulnerabilities, which suggest a non-constant atmospheric rate of decay. As climate change affects the global economy, developing an accurate model of the rate of decay becomes increasingly important in optimizing the economic and social decisions concerning consumption, investment and mitigation. The approach to specifically include carbon cycle feedbacks is new and counteracts the assumption of a constant rate of decay.

What was performed in this thesis is dynamic optimization in continuous time with an infinite time horizon. We used numerical tools to find the deterministic steady states and optimal time paths for all relevant variables in the system. A special focus was set on the mitigation variable. Three IPCC projection models, as well as the CJL model, were examined and discussed with respect to their outcomes.

The results show a rather pessimistic perspective on mitigation, where the abatement expenditure relative to the net output is low. The results even propose a smaller mitigation percentage for a higher atmospheric carbon stock. This effect is surprising, as it suggests for a fossil fuel intensive economy to release almost everything of its emissions into the atmosphere; whereas, for an economically more efficient and clean economy to hold back a greater amount of its emissions. The same difficulty is seen in the height of the social cost of carbon, which is the shadow price of an accumulating atmospheric stock of carbon.

This problem could refer to the parameters, functional forms or the insufficien-

cies in setting up the constraints for the discounted welfare function. Nonetheless, climate policy-associated decision making has to focus on the impacts derived. How policy implementation should be put through (e.g., mitigation and/or adaption) is a question of the probability of a catastrophe, a “tipping point” or an abrupt climate change [e.g., Holdren, 2008; IPCC, 2007; Pindyck, 2007; Schumacher, 2010], which for instance could be the unforeseen shutdown of the thermohaline circulation.⁷⁰

What constitutes a main aspect of criticism, is the numerical analysis, which was performed deterministically. Because of high variability across the historic annual data, we should have taken uncertainty into account. Therefore, what we recommend for further research is to leave the problem set up in this thesis as it is, but perform stochastic optimization instead.

References

Antle, J. M., and Heidebrink, G. (1995), Environment and development: Theory and international evidence, *Economic Development and Cultural Change*, 43, 603 - 625.

Barbier, E. B., and Markandya, A. (1990), The conditions for achieving environmentally sustainable development, *European Economic Review*, 34, 659 - 669.

Battle, M. L., and co-authors (2000), Global carbon sinks and their variability inferred from atmospheric O_2 and $\delta^{13}C$, *Science*, 287, 2467 - 2470.

Caldeira, K., and Wickett, M. E. (2003), Oceanography: Anthropogenic carbon and ocean pH, *Nature*, 425, 365.

Canadell, J. G., and co-authors (2007), Contributions to accelerating atmo-

⁷⁰If the latter is zero, then non-renewable resources will at all times be fully exploited. If, however, the impact of fossil use is greater, then the less non-renewable resources will be depleted [Schumacher, 2010]. Therefore, a switch will be expected to renewable resources, which are in fact more costly energy resources and are assumed to behave as perfect substitutes to the non-renewable resources [Tahvonen and Salo, 2001]. In the same way perfect substitutes could be described as constant returns to scales [Dasgupta and Heal, 1974], where both fossil as well as alternative energy could be used.

spheric CO₂ growth from economic activity, carbon intensity, and efficiency of natural sinks, *Proceedings of the National Academy of Sciences of the United States of America*, 47, 18866 - 18870.

Cesar, H., and de Zeeuw, A. (1994), Sustainability and the greenhouse effect: Robustness analysis of the assimilation function, In: J. Filar and C. Cararo (eds.), *Control and Game Theoretical Models of the Environment*, Boston: Birkhäuser.

Clarke, H. R., and Reed, W. J. (1994), Consumption/pollution tradeoffs in an environment vulnerable to pollution-related catastrophic collapse, *Journal of Economic Dynamics and Control*, 18, 991 - 1010.

Comolli, P. M. (1977), Pollution control in a simplified general-equilibrium model with production externalities, *Journal of Environmental Economics and Management*, 4, 289 - 304.

Cox, P. M., Betts, R. A., Jones, C. D., Spall, S. A., and Totterdell, I. J. (2000), Acceleration of global warming due to carbon-cycle feedbacks in a coupled climate model, *Nature*, 408, 184 - 187.

D'Arge, R. C. (1971), Essay on economic growth and environmental quality, *Swedish Journal of Economics*, 73, 27 - 43.

Daly, H. E. (1974), The economics of the steady state, *American Economic Review*, 64, 15 - 21.

Dasgupta, P., and Heal, G. (1974), The optimal depletion of exhaustible resources, *The Review of Economic Studies*, 41, 1 - 125.

Dasgupta, P. (1982), *Control of resources*. Cambridge, Massachusetts, Oxford: Harvard University Press.

Denman, K. L., and co-authors. (2007), In: S. Solomon and co-editors (eds.), *IPCC Climate Change 2007 (Fourth Assessment Report): The Physical Science Basis*, 499 - 587, Cambridge: Cambridge University Press.

Forest, C. E., Stone, P. H., and Sokolov, A. P. (2006), Estimated PDFs of climate system properties including natural and anthropogenic forcings, *Geophysical Research Letters*, 33.

Forster, B. A. (1973), Optimal consumption planning in a polluted environment, *Economic Record*, December, 534 - 545.

Forster, B. A. (1975), Optimal pollution control with a nonconstant exponential rate of decay, *Journal of Environmental Economics and Management*, 2, 1 - 6.

Forster, B. A. (1980), Optimal energy use in a polluted environment, *Journal of Environmental Economics and Management*, 7, 321 - 333.

Francey, R. J., and co-authors (1995), Changes in oceanic and terrestrial carbon uptake since 1982, *Nature*, 373, 326 - 330.

Friedlingstein, P., and co-authors (2006), Climate-carbon cycle feedback analysis results from the C^4 MIP model intercomparison, *Journal of Climate*, 19, 3337 - 3353.

Fung, I. Y., Doney, S. C., Lindsay, K., and John, J. (2005), Evolution of carbon sinks in a changing climate, *Proceedings of the National Academy of the United States of America*, 102, 11201 - 11206.

Golub, A., Narita, D., and Schmidt, M. (2011), Uncertainty in integrated assessment models of climate change: Alternative analytical approaches, In: C. Carraro (ed.), *Sustainable development series*, Fondazione Eni Enrico Mattei.

Hartwick, J. M. (1977), Intergenerational equity and the investing of rents from exhaustible resources, *American Economic Review*, 67, 972 - 974.

Heimann, M., and Reichstein, M. (2008), Terrestrial ecosystem carbon dynamics and climate feedbacks, *Nature*, 451, 289 - 292.

Hediger, W. (2009), Sustainable development with stock pollution, *Environmental and Development Economics*, 14, 759 - 780.

Hegerl, G. C., Crowley, T. J., Hyde, W. T., and Frame, D. J. (2006), Constraints on climate sensitivity from temperature reconstructions of the last millennium, *Nature*, 440, 1029 - 1032.

Holdren, J. P. (2008), Science and technology for sustainable well-being, *Science*, 319, 424 - 434.

Jehle, G. A., and Reny, P. J. (2011), *Advanced microeconomic theory*. Pren-

tice Hall.

John, A., and Pecchenino, R. (1994), An overlapping generations model of growth and the environment, *The Economic Journal*, 104, 1393 - 1410.

Jones, C. D., and Cox, P. M. (2005), Strong present-day aerosol cooling implies a hot future, *Nature*, 435, 1187 - 1190.

Keeler, E., Spence, M., and Zeckhauser, R. (1971), The optimal control of pollution, *Journal of Economic Theory*, 4, 19 - 34.

Keith, D. W., Minh, H. D., and Stolaroff, J. K. (2005), Climate strategy with CO₂ capture from the air, *Climatic Change*, 74, 17 - 45.

Knutti, R., Meehl, G. A., Allen, M. R., and Stainforth, D. A. (2006), Constraining climate sensitivity from the seasonal cycle in surface temperature, *Journal of Climate*, 19, 4224 - 4233.

Kuznets, S. (1955), Economic growth and income inequality, *American Economic Review*, 45, 1 - 28.

Lackner, K. S. (2003), A guide to CO₂ sequestration, *Science*, 300, 1677 - 1678.

Lackner, K. S. (2002), Carbonate chemistry for sequestering fossil carbon, *Annual Review Energy*, 27, 193 - 232.

Lontzek, T. S., and Narita, D. (2011), Risk-averse mitigation decisions under an unpredictable climate system, *forthcoming*, <http://www.business.uzh.ch/professorships/qba/publications/aktuell/LontzekNarita2011.pdf>, August 25th, 2011

Lontzek, T. S. (2011), Optimal carbon tax dynamics with carbon sequestration and damage uncertainty, *forthcoming*.

Le Quéré, C., and co-authors. (2009), Trends in the sources and sinks of carbon dioxide, *Nature Geoscience*, 2, 831 - 835.

Matthews, H. D., and Keith, D. W. (2007), Carbon-cycle feedbacks increase the likelihood of a warmer future, *Geophysical Research Letters*, 34.

Mercado, L. M., and co-authors (2009), Impact of changes in diffuse radiation on the global land carbon sink, *Nature*, 458, 1014 - 1017.

Metz, B., and van Vuuren, D. (2006), How, and at what costs, can low-level

stabilization be achieved? - An overview, In: H. J. Schellnhuber and co-editors (eds.), *Avoiding dangerous climate change*, Cambridge: Cambridge University Press.

Moomaw, W. R., and co-authors (2001), Technological and economic potential of greenhouse gas emissions reduction, In: B. Metz, O. Davidson, R. Swart, J. Pan (eds.), *Climate Change 2001: Mitigation; Contribution of Working III to the Third Assessment Report of the IPCC*, Cambridge: Cambridge University Press.

Nakicenović, N., and Swart, S. (2000), *Special report on emissions scenarios*. New York: Cambridge University Press.

Peylin, P., and co-authors (2005), Multiple constraints on regional CO₂ flux variations over land and oceans, *Global Biogeochemical Cycles*, 19.

Plourde, C. G. (1972), A model of waste accumulation and disposal, *Canadian Journal of Economics*, 5, 119 - 125.

Pommeret, A., and Schubert, K. (2009), Abatement technology adoption under uncertainty, *Macroeconomic Dynamics*, 13, 493 - 522.

Prentice, C., and co-authors (2001), The carbon cycle and atmospheric carbon dioxide, In: J. T. Houghton and co-editors (eds.), *Climate Change 2001: The scientific Basis*, 183 - 237, New York: Cambridge University Press.

Prieur, F. (2008), The environmental Kuznets curve in a world of irreversibility, *Economic Theory*, 40, 57 - 90.

Pyndick, R. S. (2007), Uncertainty in environmental economics, *Review of Environmental Economics and Policy*, 1, 45 - 65.

Quay, P. (2002), Ups and downs of CO₂ uptake, *Science*, 298, 2344.

Rayner, P. J., and Law, R. M. (1999), The interannual variability of the global carbon cycle, *Tellus*, 51B, 213 - 232.

Raupach, M. R., Canadell, J. G., and Le Quéré, C. (2008), Anthropogenic and biophysical contributions to increasing atmospheric CO₂ growth rate and airborne fraction, *Biogeoscience Discuss*, 5, 2867 - 2896.

Sabine, C. L., and co-authors (2004), The oceanic sink for anthropogenic CO₂, *Science*, 305, 367 - 371.

Sarmiento, J. L., Hughes, T. M. C., Stouffer, R. J., and Manable, S. (1998), Stimulated response of the ocean carbon cycle to anthropogenic climate warming, *Nature*, 393, 245 - 249.

Schumacher, I. (2010), When should we stop extracting non renewable resources?, *Macroeconomic Dynamics*, 14, 1 - 18.

Sitch, S., and co-authors (2008), Evaluations of the terrestrial carbon cycle, future plant geography and climate-carbon cycle feedbacks using five dynamic global vegetation models, *Global Change Biology*, 14, 2015 - 2039.

Smulders, S., and Gradus, R., (1993), The trade-off between environmental care and longterm growth: Pollution in three prototype growth models, *Journal of Economics*, 58, 25 - 51.

Smulders, Sjak (2008), Green National Accounting, *The New Palgrave of Economics*, Steven N. Durlauf and Lawrence E. Blume (eds.), Palgrave Macmillian, [http://www.dictionaryofeconomics.com/article?id=pde2008_G000196q=green %20national%20accounting&topicid=&result_number=1](http://www.dictionaryofeconomics.com/article?id=pde2008_G000196q=green%20national%20accounting&topicid=&result_number=1), August 25th, 2011

Solomon, S., Quin, S., and Manning, M. (eds.) (2007), *Climate Change 2007 - The physical science basis: Working group I, Contribution to AR 4 of the IPCC*. Cambridge University Press.

Solow, P. M. (1974), Intergenerational equity and exhaustible resources, *Review of Economic Studies, Symposium on the Economics of Exhaustible Resources*, 14, 29 - 45.

Sokolov, A. P., Wang, C., Hollian, G., Stone, P. H., and Prinn, R. G. (1998), Uncertainty in the ocean heat and carbon uptake and their impact on climate projections, *Geophysical Research Letters*, 25, 3603 - 3606.

Strøm, S. (1972), *Dynamics of pollution and waste treatment activities*. Oslo: University of Oslo, Institute of Economics.

Tahvonen, O., and Salo, S. (2001), Economic growth and transitions between renewable and nonrenewable energy resources, *European Economics Review*, 45, 1379 - 1398.

Tahvonen, O., and Salo, S. (1996), Nonconvexitites in optimal pollution ac-

cumulation, *Journal of Environmental Economics and Management*, 31 160 - 177.

Tahvonen, O., and Withagen, C. (1996), Optimality of irreversible pollution accumulation, *Journal of Economic Dynamics and Control*, 20, 1775 - 1795.

Toman, M. A., and Withagen, C. (2000), Accumulative pollution, clean technology, and policy design, *Resource and Energy Economics*, 22, 367 - 384.

Van der Ploeg, F., and Withagen, C. (1991), Pollution control and the Ramsey problem, *Environmental and Resources Economics*, 1, 215 - 236.

Weitzman, M. (2003), *Income, wealth and the maximum principle*. Cambridge, Massachusetts: Harvard University Press.

Yandle, B., Vijayaraghavan, M., and Bhattarai, M. (2002), The environmental Kuznets curve - A review of findings, methods, and policy implications, http://www.perc.org/pdf/rs02_1a.pdf, August 25th, 2011

Zeman, F. S., and Lackner, K. S. (2004), Capturing carbon dioxide directly from the atmosphere, *World Resources Review*, 16, 62 - 68.

August 25, 2011:

BERN, <http://www.ipcc-data.org/ancillary/tar-bern.txt>

CDIAC, http://cdiac.ornl.gov/ftp/ndp030/global.1751_2008.ems

IPCC, <http://www.ipcc.ch/>

NOAA1, ftp://ftp.cmdl.noaa.gov/ccg/co2/trends/co2_annmean_mlo.txt

NOAA2, ftp://ftp.cmdl.noaa.gov/ccg/co2/trends/co2_mm_mlo.txt

SRES, http://www.ipcc-data.org/sres/ddc_sres_emissions.html#a1b